DEVELOPMENT OF MICROSTRUCTURE IN HIGH-STRENGTH WELD DEPOSITS

By
Jer-Ren Yang
Trinity College
Cambridge

A dissertation submitted for the degree of
Doctor of Philosophy
at the University of Cambridge, November 1987.

PREFACE

This dissertation, which is submitted for the degree of Doctor of Philosophy in the University of Cambridge, describes research carried out under the supervision of Dr. H.K.D.H. Bhadeshia in the Department of Materials Science and Metallurgy, Cambridge, between October 1984 and October 1987. Except where acknowlegement and reference to previous work has been made, this work is, to my best knowledge, original and has been done without collaboration. Neither this dissertation, nor any one substantially similar to it has been or is being submitted for a degree, diploma or other qualification at any other University. This dissertation consists of less than sixty thousand words.

Jer-Ren Yang
November 1987

ACKNOWLEDGEMENT

I would like to express my deepest gratitude to Dr. H.K.D.H. Bhadeshia for his continued guidance, encouragement and support throughout the course of this study, and to Professor D. Hull for the provision of laboratory facilities at the University of Cambridge. I am also grateful to my colleagues in the Phase Transformation group, in particular Mr. S.A. Khan and Mr. A. Ashraf. I am indebted to Mrs. S.M. Barkham for her careful typing of this text.

Thanks are also extended to the technical staff of the Department, for maintenance of equipment and for technical advice, particularly Mr. J. Leader (dilatometer) and Mr. D. Nickel (transmission electron microscope).

I greatly acknowledge my wife Hsiang-Yu for her moral support during the period of my research. I also express my gratitude to my parents for their constant encouragement in the time of need.

This work is supported by the Ministry of Education, Republic of China and ESAB Ltd. (U.K.) to whom acknowledgement is also made.

To My Parents

DEVELOPMENT OF MICROSTRUCTURE IN HIGH-STRENGTH WELD DEPOSITS

Jer-Ren Yang

Abstract

The microstructure of high-strength weld deposits has been investigated using thermodynamic analysis and phase transformation theory, backed by experimental confirmation. The microstructures of both the fusion and reheated zones of multirun alloy-steel weld deposits have been studied. The transformation mechanism of acicular ferrite has been established, and a theory for reaustenitisation in steel weld deposits has also been proposed. In addition to the studies on weld metals, some model alloys were fabricated and tested in order to confirm some of the predictions made by the new theory for reaustenitisation.

All the weld metals studied in this investigation possess good hardenability. The primary microstructures of the fusion zone of these weld deposits consist mainly of acicular ferrite with very little allotriomorphic ferrite, Widmanstätten ferrite or microphases. Using transmission electron microscopy, it was confirmed that acicular ferrite had in three dimensions, a thin-plate morphology. In addition to intragranular nucleation on inclusions, acicular ferrite also nucleates sympathetically, giving rise to an interlocking formation of lenticular plates. The microstructure of the reheated zones in these multirun welds has also been examined, and found to be banded due to alloying element segregation during solidification.

It was found that the formation of acicular ferrite at any particular transformation temperature ceased as the carbon concentration of the residual austenite made further diffusionless transformation thermodynamically impossible, and that the transformation exhibits an "incomplete reaction phenomenon". The maximum extent of the acicular ferrite transformation increased with undercooling below the bainite-start temperature. The growth of acicular ferrite is consequently diffusionless, with carbon partitioning into austenite after the transformation event. In this respect, acicular ferrite is found to be identical to bainite. Its morphology differs from that of bainite simply because the former nucleates intragranularly at inclusions within large austenite grains and because of hard impingement between acicular ferrite plates nucleated on adjacent inclusions. It is concluded that acicular ferrite is in fact bainite which nucleates intragranularly within the large austenite grains typical of weld deposits.

Reaustenitisation of high-strength weld deposits, beginning with a microstructure of just acicular ferrite plus austenite, or bainite plus austenite has been studied under

isothermal conditions and in circumstances where the nucleation of austenite is not necessary. It is found that the reverse transformation from acicular ferrite (or bainite) to austenite does not happen immediately the temperature is raised (above that at which the acicular ferrite formed), even though alloy may be within the $\alpha+\gamma$ phase field. Reaustenitisation only occurs when the alloy is heated to a temperature where the carbon concentration of residual austenite exceeds the $\gamma/\alpha+\gamma$ phase boundary. Complete transformation to austenite only occurs at a temperature where the alloy composition equals the austenite equilibrium composition. These results follow directly from the mechanism of the acicular ferrite transformation and can only be explained if acicular ferrite growth is diffusionless.

A theory of kinetic isothermal reaustenitisation for starting microstructures acicular ferrite plus austenite, and bainitic ferrite plus austenite has also been proposed, and found to be in very good agreement with experimental data. It predicts that for a specific amount of reaustenitisation, the transformation time taken is governed not only by the parabolic growth rate constant of austenite but also the surface area of α/γ boundary per unit volume.

Reaustenitisation in a silicon steel has also been investigated. It is found that the last stages of reaustenitisation, which involve long-range diffusion, are tortuously slow. The decomposition of residual austenite during a slow heating has also been studied.

The microstructure of the heat affected zone adjacent to the capping layer of a multirun weld has been studied. It is found that as the austenite grain size decreases, the rate of allotriomorphic ferrite formation increases significantly.

The work provides a basis for the development of computer models for predicting the complete microstructure of steel weld deposits.

CONTENTS

NOMENCLATURE

Braces are used exclusively to denote functional relations; X{T} therefore implies that T is the argument of the function X.

α	allotriomorphic ferrite
α_w	Widmanstätten ferrite
α_a	acicular ferrite
α_b	bainite
γ	austenite
δ	delta-ferrite
α_1	parabolic thickening rate constant
Ae_3	equilibrium $\gamma/(\alpha+\gamma)$ phase boundary
Ae_1	equilibrium $\alpha/(\alpha+\gamma)$ phase boundary
Ae'_3	paraequilibrium $\gamma/(\alpha+\gamma)$ phase boundary
Ae'_1	paraequilibrium $\alpha/(\alpha+\gamma)$ phase boundary
Ar_3	upper temperature limit of the $\alpha+\gamma$ phase field during cooling
Ar_1	lower temperature limit of the $\alpha+\gamma$ phase field during cooling
Ac_3	upper temperature limit of the $\alpha+\gamma$ phase field during heating
Ac_1	lower temperature limit of the $\alpha+\gamma$ phase field during heating
T_o	temperature at which austenite and ferrite of identical composition have the same free energy
T'_o	temperature at which austenite and ferrite (with a certain amount of stored energy associated with transformation strains) of identical composition have the same free energy
W_s	Widmanstätten ferrite start temperature
B_s	bainite start temperature
M_s	martensite start temperature
t	time
T	absolute temperature
$\Delta L/L$	relative length change during isothermal transformation
ΔL_m	maximum relative length change observed during isothermal transformation

$\bar{a}_\alpha$	lattice parameter of ferrite at ambient temperature (25°C) measured by X-ray diffraction
a_α	lattice parameter of ferrite at reaction temperature
$\bar{a}_\gamma$	lattice parameter of austenite at the beginning of an isothermal transformation
a_γ	lattice parameter of austenite at any stage of an isothermal transformation
e_α	linear expansion coefficient of ferrite
e_γ	linear expansion coefficient of austenite
$\overline{X}$	average carbon concentration of alloy
X_i	concentration of alloying element i
S	amount of carbon locked up in ferrite either as carbides or in solution
k_i	partitioning coefficient for alloying element i
T_a	temperature at which acicular ferrite forms
T_γ	temperature of isothermal reaustenitisation
$T_{\gamma 1}$	minimum temperature at which reaustenitisation commences
$T_{\gamma 2}$	minimum temperature at which alloy becomes fully austenitic
V_γ	equilibrium volume fraction of austenite
X_γ	carbon concentration of austenite
X'_γ	carbon concentration of residual austenite when the formation of acicular ferrite ceases
$X_{T'_0}$	carbon concentration given by the T'_0 curve
X_{Ae_3}	carbon concentration given by the Ae_3 curve

Chapter One

General Introduction

1.1 Introduction

During the past few years welding has assumed an even greater role in the fabrication of metals, chiefly because of the development of new alloys with enormously increased strength and toughness. However, while considerable progress has been made in the development of steel weld metals largely by an empirical approach, it has become apparent that substantial further improvements were unlikely to be made with this expensive approach without paying careful attention to the development and control of weld microstructure.

The microstructure of steel weld deposits is complex, and its investigation has evolved somewhat separately from that of mainstream of steel research. Indeed, there are considerable problems in identifying microstructural constituents which differ in transformation mechanism rather than just in morphology. The large number of variables associated with the welding process has even made it difficult to quantitatively understand the microstructure. The development of the optimum microstructure also entails considerable empirical and increasingly expensive experimental work. For this reason, a properly developed model is a basic requirement for relating processing conditions to the microstructure and properties of welds. A computer model for the prediction of the microstructure of the fusion zone in low-alloy steel weld deposits has been established [1], but there are many approximations, and it needs to be refined. As to the reheated and heat affected zones, no proper model has yet been proposed, and much further research is necessary.

This work is an attempt to understand the development of microstructure in high-strength steel weld deposits, focussing on the as-deposited and reheated zones of multi-run welds. The microstructure of a steel weld deposit is first surveyed, and the respective phase transformation mechanisms are considered in detail. It will be shown later that the most desirable phase found in welds, acicular ferrite, is in fact intragranularly nucleated bainite, so a review on the bainite transformation is also presented. The reheated zone of a weld deposit undergoes reaustenitisation to varying degrees and a survey of reaustenitisation is also included. Finally, the microstructure of the heat affected zone in the parent metal is also reviewed.

1.2 Solidification Structure of Weld Deposits

Solidification in low-alloy low-carbon steel weld deposits involves the epitaxial growth of delta-ferrite (δ) from base-plate grains at the fusion boundary [2-5]. Due to the constitutional supercooling (Fig. I.1) and the high thermal gradients present in arc welding, solidification proceeds in a cellular manner [6-8]. The resulting δ-ferrite grains have an anisotropic columnar morphology, with their major axes following the direction of maximum heat flow. They grow towards the centre of the weld pool, and solute segregation occurs along their boundaries (Fig. I.2a). On further cooling, austenite (γ) allotriomorphs nucleate (Fig. I.2b) at the delta-ferrite boundaries and further anisotropic austenite growth along delta-ferrite boundaries leads to the formation of columnar austenite grains (Fig. I.2c) which closely resemble the original delta-ferrite morphology. Because of the complex nature of heat flow during arc welding, the isotherms that exist during solidification are in general differently oriented when compared with those present during the $\delta \rightarrow \gamma$ transformation [9]. In these circumstances, the columnar γ grains can curve away from the growth direction of the original δ grains. The daughter austenite grains can sometimes be finer than the delta-ferrite grains if the nucleation rate at δ/δ grain boundaries is high [1,10]. If the cooling rate, carbon level or the substitutional alloy content is sufficiently high, then γ is the first solid to form, and austenite grains grow epitaxially from the fusion boundary into the melt to form the classical columnar morphology [11-13].

Because the γ grain size is quite large (about 100μm wide, 3000 μm long in the form of a hexagonal prism) [14], nucleation both at γ boundaries and within the grains can become important during cooling of the weld deposit. The γ grain size and shape is important in determining the nature of subsequent transformation products such as allotriomorphic ferrite (α), Widmanstätten ferrite (α_w) and acicular ferrite (α_a) (to be discussed later). Bhadeshia et al. [1] have demonstrated quantitative relationships between the γ grain size and the volume fractions of allotriomorphic, Widmanstätten and acicular ferrite obtained in the as-deposited microstructure. Owing to the columnar structure, the epitaxial 'nucleation' events, and the cellular nature of the solidification front [15], Bhadeshia et al. assumed that the morphology of columnar γ grains could approximately be represented by space-filling hexagonal prisms of length 'C' and cross-sectional side length 'L/2' where $C >> L$ (Fig. I.3). This representation is an approximation, since the columnar grains often curve over long distances, due to the nature of heat flow in weld deposits. However, the importance of austenite grain size becomes clear in this representation, since [1]

(i) the volume fraction of allotriomorphic ferrite when processes at the ends of the

hexagonal prism are ignored, is related to L as

$$V_\alpha = \{8qC_1 (L - 2qC)\} /L^2 \quad (I.1)$$

where q is the allotriomorph half-thickness and C_1 is tan30°, and

(ii) the volume fraction of Widmanstätten ferrite is related to L as

$$V_w = \{C_4 G (L - 4qC_1) t_2^2/L^2\} \quad (I.2)$$

where G is the lengthening rate of Widmanstätten ferrite and t_2 and C_4 are complicated functions of nucleation rate etc.

Several authors [16-19] have suggested that an increase in inclusion content should, owing to boundary pinning, lead to a decrease in the γ grain size of a weld deposit. The volume fraction of inclusions in a weld is known to correlate directly with the total oxygen content of the weld [17,20] since most of the oxygen is present in the form of oxides. Harrison et al. [16-19] reported experiments in which welds with different oxygen concentrations were *reheated* into the γ phase field, and held there to allow grain coarsening. The resulting equiaxed γ grains were found to decrease in size with increasing oxygen content. However, this is not relevant to the as-deposited weld microstructure because their experiments deal with reheated weld metal, the γ grain size being controlled by a coarsening reaction driven by the γ/γ surface energy per unit volume, a driving force amounting to only a few $Jmol^{-1}$. The driving force for the formation of γ from δ-ferrite on the other hand is relatively large, and increases indefinitely with undercooling below the equilibrium transformation temperature; pinning by inclusions cannot be effective in such circumstances. It should also be noted that even if the columnar γ grains form directly from the melt by cellular solidification, the cell size at the solid-liquid interface is determined by interface stability [15] in the concentration field ahead of the interface. Oxide and other inclusions which are present in the liquid become passively included in the solid by being trapped at the advancing interface, and do not seem to play any role in influencing the cell size.

In recent research [1,2], there is strong evidence that oxygen content (121 to 418 p.p.m. by weight) does not determine the size of austenite grains in the as-deposited microstructure.

1.3 Transformation from Austenite in Steel Weld Deposit

There is a considerable literature about the study of alloy steel weld deposits. However, some of the terminology on microstructures in weld metal, which has been used in research institutes or industries, is ambiguous. For example, allotriomorphic ferrite (Dubé classification[21]) is sometimes called "grain boundary proeutectoid ferrite" or just "grain boundary ferrite", but these terms fail to distinguish between Widmanstätten ferrite and allotriomorphic ferrite, both of which can form above the eutectoid temperature and at austenite grain boundaries. This literature survey is intended to describe the morphologies of microstructures in weld metals and to summarise their transformation mechanisms where they are known. In a typical steel weld metal, the phases consist of allotriomorphic ferrite, Widmanstätten ferrite, acicular ferrite, idiomorphic ferrite, microphases and inclusions,etc.

1.3.1 Allotriomorphic Ferrite (α)

Allotriomorphic ferrite (α) is the first phase to form during the cooling of low-alloy steel weld deposits to temperatures below the Ae_3 temperature [22-24]. The ferrite usually nucleates heterogeneously at the boundaries of the columnar austenite grains, and these boundaries rapidly become decorated with virtually continuous layers of polycrystalline ferrite. The morphology of this ferrite is like a layer and does not reflect its crystal symmetry [25]. Many of the grains are expected to have a rational orientation relationship with one of adjacent austenite grains.

In plain carbon steels, allotriomorphic ferrite is a dominant phase over wide ranges of composition and temperature. Classically, it used to be the view [26,27] that transformation occurs with α nuclei forming a partially coherent interface with only one adjacent austenite grain, while a random relation exists with the other. The well matched interface, possessing low energy, is then postulated to move by the displacement of ledges; while the other relatively higher energy interface is supposed to be displaced by the continuous motion of the whole interface. It is now known that a ferrite nucleus can have rational orientation relationships with both the adjacent austenite grains in some cases, as pointed out by Hillert [28]. The growth of α has been shown [29,30] in general to be a diffusion-controlled process.

In the case of weld deposits, which generally contain a very low carbon and substitutional alloy content in order to avoid cold cracking, the time for α to saturate the γ boundaries is so small that the formation of much of the α essentially involves the diffusional thickening of layers of grain boundary allotriomorphic ferrite [31]. For this reason, it is reasonable to model this transformation simply in terms of growth (Fig. I.4a)

with the growth occurring by the normal migration of planar austenite-ferrite interfaces, leading to the thickening of the layer of α.

If it is assumed that the growth of the layers of α is diffusion-controlled (diffusion of carbon in austenite), and that for alloy steels the transformation occurs under paraequilibrium conditions [32], then for isothermal transformation the volume fraction of allotriomorphic ferrite (V_α) should mainly depend on the parabolic rate constant α_1, defined [33] by the equation:

$$q = \alpha_1 \, t^{0.5} \tag{I.3}$$

where q is the allotriomorphic ferrite half-thickness and t is the time, defined to be zero when q = 0. Most steel weld deposits are at least quartenary alloys, and the diffusion control could arise from the diffusion of carbon or of substitutional alloying elements [34]. However, for alloys higher than ternary alloys, the complexity of treating multi-component diffusion is beyond reason [35]. It is noted that the growth of α in dilute steels occurs without the bulk partitioning of substitutional elements [36], especially when the growth rates involved are large [34,37], as is the case for weld deposits. In these circumstances, ferrite growth can occur at a rate controlled by diffusion of carbon in the austenite ahead of the interface. Bhadeshia et al. [31] have assumed that α growth occurs by a carbon diffusion-controlled paraequilibrium mechanism [32] so that substitutional elements do not partition at all between the phases; subject to this constraint, carbon partitions to an extent which allows its chemical potential to be identical in all phases. It is believed [31] that for low-alloy steel weld deposits, most of the variation in volume fraction of allotriomorphic ferrite (V_α) as a function of composition can be rationalised in terms of the parabolic thickening rate constant α_1. Having calculated q, the volume fraction of allotriomorphic ferrite (V_α) is given, from geometrical considerations by equation I.1.

$$V_\alpha = \{8qC_1 \, (L - 2qC)\}/L^2 \tag{I.1}$$

However, the above theory consistently underestimates the amount of allotriomorphic ferrite. That procedure works well if the calculated volume fraction is multiplied by a factor of about two [1], as presented in equation I.4:

$$V_\alpha = 2.04 \, [8qC_1(L-2qC)/L^2] + 0.035 \tag{I.4}$$

Evidently, the major assumption, which causes underestimation, is that γ boundaries become decorated uniformly with a thin layer of α, the α then subsequently thickening

normal to the γ grain boundary. In some relatively heavily alloyed welds this is unjustified since discontinuous layers of α are observed [38]. Even when uniform and continuous layers of α are observed, the early stages must involve a faster rate of transformation since growth is initially not confined to one dimension. It is only when site-saturation follows that the model of one dimensional allotriomorph thickening should be a good approximation.

Recently, Bhadeshia et al. [39] have presented a new model (Fig. I.4b) in which the allotriomorphs prior to site-saturation are modelled as discs parallel to the austenite grain boundary planes. Because allotriomorphic ferrite formation is complete within a few seconds, soft impingement between allotriomorphs growing from opposite grain boundaries should not occur and this method takes account of hard impingement. This analysis has been shown to be a better approximation and is also independent of the γ grain shape. The following equation shows the relations for this model [39].

$$- \ln \{1 - \zeta\} = (2 S_v/\phi) (\alpha_1 t^{0.5}) f \{\theta, \eta\alpha_1, I_B, t\} \qquad (I.5)$$

where ζ = the volume of allotriomorphic ferrite (α) divided by its equilibrium volume,

S_v = surface area of α per unit volume,

ϕ = volume fraction of α at equilibrium,

η = ratio of length to thickness of allotriomorph,

α_1 = parabolic rate constant, and

$f \{\phi, \eta\ \alpha_1, I_B, t\}$ is a complicated function of parabolic rate constant and grain boundary nucleation rate per unit area etc.

This new theory has been developed to allow the calculation of the volume fraction of allotriomorphic ferrite in welds, even when site saturation does not occur at an early stage of transformation.

The formation of fairly uniform layers of allotriomorphic ferrite at the columnar austenite grain boundaries is generally accepted to be detrimental to toughness [40-42]. The continuous layers of such ferrite seem to offer little resistance to crack propagation. Increasing the hardenability of weld metal by addition of alloy elements such as Mn, Cr, Ni or Mo to filler metal substantially decreases the amount of allotriomorphic ferrite to the point of extinction. It would be interesting to investigate the optimum alloy addition by alloy design.

1.3.2 Widmanstätten Ferrite (α_W)

It is believed [41,43,44] that during continuous cooling, the transformation temperature of α_W is just below that of allotriomorphic ferrite. In a typical steel weld deposit, there are usually two kinds of Widmanstätten ferrite to be found. Secondary Widmanstätten ferrite nucleates at the allotriomorphic ferrite-austenite boundaries and grows as sets of parallel plates separated by thin regions of austenite, the latter subsequently being retained to ambient temperature or partially transforming to martensite and/or pearlite. These small quantities of retained-austenite, martensite and degenerate pearlite mixtures are called "microphases" [45]. The Welding Institute therefore refers to this Widmanstätten ferrite and its associated microphases as "Ferrite with Aligned Martensite-Austenite-Carbide"[45]. Primary Widmanstätten ferrite can nucleate directly from austenite grain boundaries which are not covered by allotriomorphic ferrite, although its growth mechanism is identical to that of Secondary Widmanstätten ferrite. Widmanstätten ferrite was also thought to form within prior austenite grain [46], and Dubé had classified this morphology as intragranular Widmanstätten ferrite [21]. However, there is still no conclusive evidence for this in terms of serial sectioning experiments, and it is suggested that α_W growth from allotriomorphic ferrite or from austenite grain boundary is favourable.

On an optical scale, α_W possesses a plate shape with a thin wedge section [47]. The formation of α_W is also accompanied by a shape change [47,48], the shape change due to a single wedge of Widmanstätten ferrite consisting of two adjacent and approximately opposite invariant-plane strain deformation. The surface relief of α_W transformation supports the view that in the process of α_W growth, atomic correspondence is maintained at least for substitutional atoms. In steel weld deposits, α_W plate has an apparent aspect ratio (length/thickness) of 20/1 or greater [49,50], but there are no quantitative data about its length and thickness. Bhadeshia [41] has measured the average length and thickness of α_W in Fe - Ni - Si - C steel, and the mean values were found to be about 156 μm and 1.4 μm respectively, after considering sectioning effects. Using the aspect ratio, the shape strain data and elastic constants, the strain energy of α_W has been calculated [47] as about 50 J/mol. At high temperatures, it is impossible for the ferrite plate to grow on its own, since the strain energy due to the shape change would far exceed the available driving force. Hence the reaction involves the simultaneous and adjacent co-operative growth of two plates, which are crystallographic variants whose shape changes cancel each other, drastically reducing the strain energy term. Both the adjacent variants of Widmanstätten plate have been known to possess a rational KS-NW type orientation relation with austenite [25]. Because α_W forms at the low undercoolings, the diffusion of carbon during growth is thermodynamically necessity; however this redistribution of carbon does not

affect the shape change or the displacive* [51] character of the transformation. It is believed [47] that α_w always has an equilibrium carbon content and grows at a constant rate controlled by the diffusion of carbon in the austenite ahead of the plate tip.

In the microstructure of low-carbon low-alloy steel weld metals, the volume fraction (V_w) of Widmanstätten ferrite can be estimated by considering the Widmanstätten ferrite to nucleate at α/γ boundaries and grow into the interior of the columnar austenite grains; the latter are again assumed to be hexagonal prisms and end effects are neglected. Assuming that the α_w nucleation rate per unit area of α/γ interface is constant, the volume fraction of Widmanstätten ferrite is given by [10]

$$V_w = \{C_4\, G\, (L - 4q'C_1)\, t_2^2/L^2\} \qquad \text{(I.6)}$$

where C_4 = a constant independent of alloy composition,
G = lengthening rate of α_w,
$L/2$ = cross-sectional side length of hexagonal austenite grain,
q' = a corrected value of α thickness,
t_2 = the time interval in which α_w grows.

As to the mechanical properties, α_w in weld deposits is generally regarded as an undesirable constituent because it is believed to lead to poor fracture toughness [40,52].

1.3.3 Acicular Ferrite (α_a)

Acicular ferrite has been known to be the most desirable microstructural consistent in steel weld metals because its presence directly correlates with improved toughness [53,55]. However, acicular ferrite is not included in the Dubé classification [21], and is not in general found in wrought steels. α_a is characterised by fine elongated platelets of ferrite arranged in an interlocking pattern [40], i.e., non-parallel plates within the columnar austenite grains. It has been suggested that most of acicular ferrite is about 1μm thick [56], and with an apparent aspect ratio (length/thickness) of 3/1 - 10/1, but these measurements do not account for stereological errors. Some authors [56-58] have proposed that the orientation between adjacent acicular ferrite plates results in a "high-angle" interface between the plates. Ito et al. [57] showed the angle was 26° in their research. It is noted that the orientation relation should include both an axis and an angle to form a complete description [59]. Some authors [56,58] have also suggested that individual acicular ferrite plates contain a relatively high dislocation density, however,

* In interstitially alloyed materials, the substitutional lattice can maintain an atomic correspondence while the interstitials diffuse; this is displacive transformation.

there are no quantitative data on this. It would be interesting to examine in detail the orientation relation and boundary structure between adjacent variants, and dislocation density of acicular ferrite as compared with other transformation products. It is believed [60,61] that acicular ferrite nucleates intragranularly at inclusions, and it has also been suggested [62] that the fine interlocking nature of acicular ferrite is due to sympathetic nucleation [63] of ferrite, during which the austenite/ferrite interface could also become an active nucleation site for further ferrite transformation.

The transformation mechanism of acicular ferrite [64,65] has now been studied in detail. Acicular ferrite seems to be bainite which nucleates intragranularly within the large columnar austenite grains. The acicular ferrite plates form by a diffusionless and displacive transformation mechanism, and immediately after plate growth, carbon is partitioned into the residual austenite. Acicular ferrite differs morphologically from classical sheaf-like bainite simply because acicular ferrite nucleates intragranularly at point sites, and is limited also by hard impingement with other plates which form on neighbouring sites. In relatively pure alloy not containing large numbers of inclusions, the bainite nucleates from austenite grain boundaries and classical bainite sheaves form. Acicular ferrite requires the presence of inclusions to enable intragranular nucleation, and will only form when the austenite grain size is relative large, so that events originated from the grain boundaries do not swamp those occurring intragranularly. Intragranular nucleation on inclusions has a higher activation energy compared with grain boundary nucleation [66] so that the number of grain boundary site must be minimised to obtain acicular ferrite. The results on thermodynamics of acicular ferrite transformation in alloy-steel weld deposit are presented in Chapter Three.

1.3.4 Inclusions

Inclusions in weld metals primarily originate from oxides formed during weld deposition, or from the unintentional trapping of slag forming materials (silicates and sulphides) which are used to protect the molten metal during welding. The mean inclusion diameter in low-alloy steel weld deposit can typically be about 0.3μm [60,61], although some inclusions as large as 1μm [67] are sometimes found. The size distribution of inclusions, together with volume fraction measurement, can be realistically determined by using replica techniques and the electron microscope, because 0.3μm inclusion size is at the lowest limit of resolution of optical microscope. The inclusions in welds probably comprise mixed oxides, nitrides, silicates or sulphides which could contain Fe, Mn, Ti, Al, B, Mg, and Ca etc. [61,62,68]. The chemical compositions of inclusions are very complicated, depending on the processes of fusion welding. Generally the volume fraction of inclusions correlates with the total oxygen content of the weld, because most of the

oxygen is present in the form of oxides and most of the inclusions are oxides. Inclusions act as stress concentrators and crack nucleation sites [69] in weld metals, so their content should be kept to a minimum. On the other hand, it is also believed that they may serve as nuclei for the formation of acicular ferrite, a most desirable phase from the point of view of toughness. In order to reach an optimum inclusion content with the right size distribution, it is essential that a method is developed for quantitatively predicting the important characteristics of inclusions in welds.

Recently, it has been found [70] that in steel weld metals relatively large inclusions segregate preferentially, during solidification, to the columnar grain boundaries of the first phase to solidify, whether this is δ-ferrite or austenite. For a steel solidifying as δ-ferrite, the subsequent transformation to austenite would cause the inclusions to finish up in or near the centre of the columnar austenite grains. It should also be noted that the high cooling rates associated with most arc-welding processes causes non-equilibrium solidification so that the final weld is compositionally heterogeneous. The influence of such segregation relative to the position of the inclusions on the final microstructure should be rather important. However, the subject has not yet been studied.

Ito et al. first proposed [71] that the microstructural component present in a given steel weld metal was dependent on the oxygen content. They showed that in Fe-Si-Mn-Ti-B weld metal, at an intermediate oxygen level (270ppm) acicular ferrite structure was formed, while bainitic ferrite structure was apt to appear at low oxygen levels (60ppm), and allotriomorphic ferrite and Widmanstätten ferrite were formed predominantly at higher oxygen contents (440ppm), although there is no evidence at present whether inclusions enhance the grain boundary nucleation rate of allotriomorphic ferrite and Widmanstätten ferrite as well. Some authors [56,60,72] have proposed that the surface energy between the matrix and inclusion (composition, coherency and crystallinity considerations) and the high strains developing around particles during weld metal shrinkage on cooling are likely to enhance ferrite nucleation. It is expected in this respect that more detailed information will become available as analytical techniques progress.

1.3.5 Microphases

The microphases in weld metals correspond to carbon rich regions, which are the last volumes of austenite to transform. Microphases can be found among the non-parallel plates of acicular ferrite, and appear as fine dispersions of islands [73] under the light microscope. On the other hand, thin layer like microphases are located between the parallel plates of Widmanstätten ferrite, and the Welding Institute therefore refers to this Widmanstätten ferrite and its associated microphases as "Ferrite with Aligned Martensite-Austenite-Carbide" [45,74]. It is reasonable to conclude that the microstructures of

microphases depend upon the degree of carbon enrichment. Rejection of carbon by the growing ferrite grains stabilises the surround austenite. Eventually, after mutual impingement of ferrite grains, entrapped austenite transforms to martensite of degenerate pearlite or is retained to ambient temperature. The volume fraction of microphases may be estimated by equating it to the amount of austenite remaining untransformed at the M_S temperature. There is no quantitative information about how the microphases influence the properties [74-76], but it is evident that a large volume fraction of microphases should be detrimental to the toughness of the weld metals.

1.3.6 Idiomorphic Ferrite

Idiomorphic ferrite [21] has a roughly equiaxed morphology, and usually forms intragranularly, presumably at inclusions or other heterogeneous nucleation sites. Idiomorphic ferrite is also sometimes thought to form [46,74] in steel weld metal (often classified as "intragranular polygonal ferrite"). However, there is no systematic work to prove that the observed effects do not arise as a consequence of sectioning effects. In any case the amount of idiomorphic ferrite reported in normal Fe-C-Mn-Si weld metals is very small or completely absent.

1.4 Model of Microstructure in Weld Deposits

A convincing model for the prediction of the microstructure of the fusion zone of steel welds has been proposed by Bhadeshia et al. [1,31,77-79]. This model has been tested successfully for Fe-C-Si-Mn, Fe-C-Si-Mn-Cr, Fe-C-Si-Mn-Mo and Fe-C-Si-Mn-Ni alloy steel welds. A brief description of this model is given below.

In this model the morphology of prior austenite grains it is assumed can be approximated as hexagonal prisms. Fig. I.5 illustrates schematically the development of microstructure in the low-alloy and high-alloy weld deposits. The hexagons represent cross-sections of columnar austenite grains whose boundaries first become decorated with a uniform layer of polycrystalline allotriomorphic ferrite (α) and Widmanstätten ferrite (α_w) growth follows later. Depending on the growth rate of α_w, the α_w then impinges with α on the opposite boundary in the case of low-alloy deposits, or with acicular ferrite (α_a) nucleated on inclusions (black dots) in the case of relatively high-alloy deposits. The microphases originate from the decomposition of residual austenite, which was originally between the interlocking acicular ferrite plates or between the parallel Widmanstätten ferrite plates.

The flow chart (Fig. I.6) demonstrates the steps involved in the calculation of the microstructure for this model. At first, it requires an input of chemical composition, the

austenite grain parameters and the cooling curve of the weld deposit [73], over the temperature range 800→500°C. Having established the input data, the next step involves the calculation of a multicomponent phase diagram, time-temperature-transformation (TTT) and continuous-cooling transformation (CCT) curves, which when combined with the cooling rate equation [77] gives the various reaction-start and finish temperatures. T_h and T_l are the temperatures at which allotriomorphic ferrite formation begins and ends respectively, and M_S, B_S, W_S are the thermodynamically calculated martensite, bainite and Widmanstätten ferrite start temperatures respectively. The volume fraction of allotriomorphic ferrite can be predicted by assuming the paraequilibrium thickening of layers of ferrite [1], and is given by equation I.4. Widmanstätten ferrite is the next phase to grow on further cooling and its volume fraction V_w is given by equation I.6.

$$V_\alpha = 2.04\,[8qC_1(L - 2qC)/L^2] + 0.035 \qquad \text{(I.4)}$$

$$V_w = C_4G\,(L - 4qC_1)t_2^2/L^2 \qquad \text{(I.6)}$$

where q is the half-thickness of the α layer at the γ grain boundaries, G is the α_w growth rate and t_2 is the time during which α_w grows. In the flow chart, t_1 is the time available for α growth, and t_3 is the time required for an α_w plate to grow across a γ grain, given by:

$$t_3 = (L \sin 60^\circ - 2q)/G \qquad \text{(I.7)}$$

To account for physical impingement between α_w and α_a, a further time interval t_c is defined; if $t_3 < t_c$, α_w growth occurs essentially without impingement and $t_2 = t_3$. If on the other hand $t_3 > t_c$, then $t_2 = t_c$, and α_w plates can only grow to a length Gt_c before growth is terminated by physical impingement with α_a plates. The t_c value can be determined by fitting eqs. I.4, 6 and 7 to data from one weld.

The microphases originate from the decomposition of residual austenite to degenerate pearlite and/or martensite, and their volume fraction (V_m) may be estimated by equating it to the amount of austenite remaining untransformed at the M_S temperature. The quantity of γ can be calculated by assuming that α, α_w and α_a form to the maximum extent specified by the lever rule as applied to the Ae_1 and Ae_3' lines at the M_S temperature. Hence, it is assumed that ferrite formation proceeds until the carbon content of the residual austenite reaches Ae_3', so that V_m in general represents the minimum possible estimate of microphase content. This should be a good approximation for the low-alloy steels since the rate of transformation is very high. After estimating V_m, the volume fraction of acicular ferrite (V_a) can be calculated by:

$$V_a = 1 - V_\alpha - V_w - V_m \qquad (I.8)$$

Published experimental data on the variation of microstructure have been analysed using this model for the development of microstructure in low-alloy steel weld deposits [1,31,77-79]. Although this model is in many ways approximate, the results are on the whole in good agreement with theory. However, it will still be necessary to refine the model in the light of further experimental results and theoretical developments.

1.5 Role of Alloying Elements in Transformation Kinetics

The composition of weld metals is decided by many factors, including the composition of the filler wire, factors such as dilution from the base plate, flux chemistry, sheilding gases etc. However, typically the final composition of deposit lies between that of the filler metal and the base metal. In structural steels, the CCT (continuous cooling transformation) curves or TTT (isothermal time-temperature-transformation) curves can effectively be controlled by careful choice of alloying elements. The effects of alloying elements on the hardenability of steel is related directly to their effects on the nucleation and growth kinetics of allotriomorphic ferrite and other austenite decomposition products. Usually the kinetics of the allotriomorphic ferrite transformation is a principal consideration.

The study of the growth kinetics of allotriomorphic ferrite in Fe-X-C ternary system (X is a substitutional alloying element) has been the subject of a great deal of interest in the past two decades [80]. The effect of alloying elements on the transformation of austenite [34,80-83] has been studied considering the behaviour of an alloying element in and close to the moving interface. The rate at which an interface moves depends both on its intrinsic mobility (related to the process of atom transfer across the interface) and on the ease with which any alloying element partitioned during transformation diffuses ahead of the moving interface [25]. Both of these processes dissipate the free energy (ΔG) available for interface motion; when ΔG is mainly used up in driving the diffusion of solute ahead of the interface, growth is said to be diffusion-controlled. On the other hand, interface-controlled growth occurs when most of ΔG is dissipated in the process of atom transfer across the interface.

These concepts can be easily illustrated in terms of the formation of allotriomorphic ferrite from supersaturated γ in a Fe-C alloy isothermally transformed in the $\alpha + \gamma$ phase field at a temperature T. The notation used is defined as follows: the mole fraction of an element i (i = 1,2,3 for C,X,Fe respectively, where X is a substitutional alloying element) in a phase α at the α/γ interface is written χ_i^α, with $\chi_i^{\alpha\gamma}$ representing the mole fraction of

i in α, when α is in equilibrium with γ. In the same manner, χ_i^{γ} and $\chi_i^{\gamma\alpha}$ are defined. $\bar{\chi}_i$ refers to the average mole fraction of i in the alloy concerned. For isothermal growth of ferrite of composition $\chi_1^{\alpha\gamma}$ involving the movement of a flat α/γ interface, the total composition difference between the ferrite and austenite remote from the interface may be written [25]:

$$\Delta\chi = \Delta\chi_{\infty} + \Delta\chi_I + \Delta\chi_D \qquad (I.9)$$

where
$$\Delta\chi_{\infty} = \chi_1^{\gamma\alpha} - \chi_1^{\alpha\gamma}$$
$$\Delta\chi_I = \chi_1^{\gamma} - \chi_1^{\gamma\alpha}$$
$$\Delta\chi_D = \bar{\chi}_1 - \chi_1^{\gamma}$$

$\Delta\chi_{\infty}$ is the difference of mole fraction of carbon between γ and α in the equilibrium state. $\Delta\chi_I$ and $\Delta\chi_D$ are related to the free energies G_I and G_D dissipated in the interface and diffusion processes, respectively, such that $G_D = 0$ when $\Delta\chi_D = 0$ and $G_I = 0$ when $\Delta\chi_I = 0$. Similarly, ΔG is related to $(\Delta\chi_{\infty} - \Delta\chi)$ and is zero when $\chi_1^{\gamma\alpha} = \bar{\chi}_1$.

Actually the rate of interface motion is always under mixed control (since the two processes are in series) but it is said to be diffusion controlled if $|\Delta\chi_D| >> |\Delta\chi_I|$ and because variations in interface parameters have virtually no effect on velocity. In the same way, interface control implies that $|\Delta\chi_D| << |\Delta\chi_I|$ and variations in diffusion parameters then have a negligible effect. True mixed control implies that $\Delta\chi_D$ and $\Delta\chi_I$ are of comparable magnitude.

The diffusional growth of allotriomorphic ferrite (α) during transformation in the $\alpha+\gamma$ phase field involves the partitioning of carbon. If it is considered that the interface moves at a rate which is under mixed diffusion- and interface-control, then a possible carbon concentration profile developed at the α/γ interface can be illustrated in Fig. I.7. However, a reasonable approximation for diffusion-controlled growth is that the compositions of the phase in contact at the interface are in equilibrium. This is because $\Delta\chi_I$ is relatively small for diffusion-controlled growth. Subject to this approximation, local equilibrium is said to exist at the interface. This involves the assumption that the whole of the concentration gradient can be divided up into a large number of thin slices (or sub-systems), each of which has a definite concentration, so that each of the sub-systems can be considered as if it were in local equilibrium. These assumptions are valid if perturbations from equilibrium are not too large [84] and they allow the application of classical equilibrium thermodynamics to steady-state situations like the irreversible process of diffusion which actually arises due to the lack of equilibrium. It is a common assumption that we may apply equilibrium thermodynamics locally [85].

In Fe-X-C ternary systems (X is a substitutional alloying element), the diffusion-controlled growth is complicated by the fact that both interstitial and substitutional atoms diffusion occurs during transformation. The respective diffusion coefficients differ substantially and this combined with the assumption of local equilibrium at the interface leads to a variety of possible growth modes [34,35,80-83]. These models are discussed as follows.

1.5.1 Diffusion-Controlled Growth of Ferrite in Fe-X-C Alloy: Local Equilibrium

During ferrite growth with local equilibrium, the composition of the ferrite (α) and austenite (γ) at the interface can be connected by a tie-line of $\alpha+\gamma$ phase field in the equilibrium Fe-X-C phase diagram. This tie-line which defines the interface composition does not in general pass through the point in the $\alpha+\gamma$ phase which identifies the alloy composition. This is because the diffusivities of interstitial (C) and substitutional alloying elements (X) in the γ are significantly different. The appropriate tie-line must be chosen to satisfy mass conservation conditions at the moving interface and must be consistent with the partitioning behaviour of the alloying elements. Therefore, the tie-line for an alloy transforming at a low supersaturation is such that there is considerable partitioning and long-range diffusion of substitutional alloying element, while the driving force for carbon diffusion is reduced to a level which allows the substitutional element flux to keep pace with the carbon flux at the interface [25]. This situation [34] is referred to as the partitioning under local equilibrium condition (P-LE), as shown in Fig. I.8a.

On the other hand, at higher supersaturations the determining tie-line cause negligible partitioning of substitutional alloying element (X) between the α and γ phases, so that the gradient of the X element in the γ near the interface is very large. This drastically increases the driving force for X diffusion in γ and allows the flux of X to keep up with the long-range diffusion of carbon in γ [25]. In this situation, the diffusion of substitutional alloying element (X) is extremely short-range, being confined to the immediate vicinity of the interface. This condition [34] is designated as the negligible partitioning under local equilibrium (NP-LE), as presented in Fig. I.8b.

The schematic isothermal equilibrium Fe-Mn-C system phase diagram (Fig. I.8c) shows a division of the $\alpha+\gamma$ phase field into domains where either the P-LE or the NP-LE mechanism can operate [25,34]. It should be noted that both of these modes of transformation involve local equilibrium at the interface and are therefore equally favoured on the thermodynamic considerations. Both carbon and substitutional elements diffuse during growth and their fluxes should satisfy the equations for conservation of mass at the interface. Hence the interface velocity calculated from diffusion of C in γ will be identical to that calculated from diffusion of Mn in γ. Both elements control the

growth rate and neither can be said to restrict the interface motion independently.

1.5.2 Diffusion-Controlled Growth of Ferrite in Fe-X-C Alloys: Paraequilibrium

Kinetic factors can prevent the transformation from occurring under equilibrium conditions. Such a case could arise, for example, when a phase change is so rapid that one or more of the components cannot redistribute among the phases in the time scale of experiment. For transformations in steels, the diffusion coefficients of substitutional and interstitial component differ so greatly that it is possible to imagine circumstances where the sluggish substitutional alloying elements may not have sufficient time to redistribute during transformation of γ to α, even though carbon may partition into the austenite.

The term "paraequilibrium" has been introduced [34,37,86] to describe at very high supersaturations a kinetically constrained equilibrium where the two adjoining phases have identical X/Fe atom ratio, but subject to this constraint, carbon is redistributed so that its chemical potential is identical in both phases at the interface. In other words, ferrite formation under the condition of paraequilibrium implies that the substitutional lattice is configurationally frozen and if interface processes are not limiting, the transformation occurs at a rate controlled by the diffusion of carbon in the austenite. Thus, the chemical potentials of the substitutional elements are not equal in the two phases, but carbon which diffuses faster reaches equilibrium subject to this constraint. Typical paraequilibrium and equilibrium Fe-Mn-C diagrams are illustrated in Fig. I.9. It is clear that for any given alloy, a critical undercooling below the equilibrium transformation temperature is necessary before paraequilibrium transformation become feasible. This is because of the fact that a relatively low free energy change accompanies the formation of ferrite which is forced to accept a non-equilibrium substitutional alloy content. It is also noted that the paraequilibrium boundaries project to the binary equilibrium on the Fe-C side and to the T_0 composition (the point where γ and α of the same composition have the equal free energy) on the Fe-X side.

1.6 The Bainite Transformation in Steels

Acicular ferrite in weld metal seems to be intragranularly nucleated bainite. It would be useful to have a review on the bainite transformation, before presenting the study of acicular ferrite formation. Christian and Edmonds [87] have provided an excellent survey of the bainite transformation regarding the microstructure and the transformation mechanism in steels, which will form a framework for the present review.

1.6.1 TTT Diagram and Isothermal Transformation Curve

Bainite forms by the decomposition of austenite at a temperature above the Ms temperature, but below that of fine pearlite. In low alloy steels, the pearlitic and bainitic temperature ranges overlap each other to a considerable extent, and this makes the interpretation of microstructure and kinetics very difficult. However, in medium alloy steels, the isothermal time-temperature-transformation (TTT) diagram possesses two separate C curves; in such a diagram, the upper C curve represents the time taken for the initiation of diffusional transformations such as allotriomorphic ferrite and pearlite, whereas the lower C curve represents the time taken for the initiation of the Widmanstätten ferrite or bainite transformation. The lower C curve usually exhibits a flat top, which corresponds to the Bs (bainitic start) temperature.

An interesting feature of the isothermal bainite transformation is the existence of the "incomplete reaction phenomenon" [88,89]. At any temperature within the bainite transformation range, and in the absence of any interfering secondary reactions, only a limited quantity of bainitic ferrite forms before the reaction terminates. This apparently premature termination occurs before the carbon content of the remaining austenite reaches the equilibrium level indicated by the extrapolated Ae_3 curve. The maximum extent of transformation that can be achieved increases with undercooling below the Bs temperature.

1.6.2 Microstructure

Bainite is essentially a non-lamellar aggregate of plate-shaped ferrite and carbides. The carbide part of the microstructure is not essential to the transformation and in many cases, for example, upper bainite in silicon steel, carbides are totally absent [90]. The ferrite plate size is typically about 10μm long, with a thickness of about 0.2μm [84]. There are two classical morphologies of bainite: upper bainite and lower bainite.

Upper Bainite

Upper bainite consists of platelets of ferrite adjacent to each other, which are in very nearly the same crystallographic orientation in space, so that wherever two adjacent platelets touch, a low angle boundary arises. Elongated cementite particles usually decorate the boundaries of these platelets, the amount of these slabs of cementite depending on the carbon content of the steel. These ferrite platelets, which form a sheaf, have the same habit plane [91-93], and the sheaf itself has a thin wedge plate morphology in three-dimensions on a macroscopic scale [89]. Sheaves of upper bainite inevitably nucleate at prior austenite grain boundaries, and intragranular nucleation is not to be

found. The slabs of cementite (θ) actually form from the austenite between the ferrite platelets, and hence do not have a rational orientation with the ferrite, but have a Pitsch [94] relation with the austenite, i.e.,

$$(001)_\theta \quad // \quad (\bar{2}25)_\gamma$$
$$[100]_\theta \quad // \quad [5\bar{5}4]_\gamma$$

The bainitic ferrite after transformation may retain a small supersaturation of carbon, and has a rational orientation relationship with the austenite.

In silicon-containing steels, Bhadeshia et al. [89] have shown that sub-units within a sheaf of upper bainite can also be distinguished where no carbides form but where the ferrite plateles are separated by films of carbon-enriched retained austenite.

Lower Bainite

Lower bainite is basically very similar to upper bainite, except that the amount of interplate cementite is less, and carbide can additionally be found within the ferrite plate itself. These intra-ferrite carbides can be epsilon carbide in the case of high carbon steels or cementite in case of low carbon steels. It has been estimated [95] that epsilon carbide will not be formed in bainitic ferrite for steels with a carbon content below approximately 0.55 wt%. The carbide particles usually precipitate in a single crystallographic orientation such that their habit plane is inclined at about 60° to the plate axis. In some cases, several variants have been observed [95,96] although the 60° variant still tends to dominate. The inter-plate carbide does not necessarily exist, and results from the diffusional decomposition of carbon-enriched austenite which has not transformed to ferrite. The intra-ferrite cementite precipitated in a single variant has a Bagaryatskii [97] orientation relationship with ferrite, identical to that found when martensite is tempered, i.e.,

$$[100]_\theta \quad // \quad [0\bar{1}1]_\alpha$$
$$[010]_\theta \quad // \quad [1\bar{1}\bar{1}]_\alpha$$
$$[001]_\theta \quad // \quad [211]_\alpha$$

The orientation relation between lower bainitic ferrite and austenite is close to either the Kurdjumov-Sachs [98] or the Nishiyama-Wasserman [99] orientation. The ferrite also forms as sheaves, so that very low angle boundaries arise between platelets within a sheaf.

1.6.3 Carbides Formation during the Bainite Transformation

It is essential that the nature and significance of carbide precipitation accompanying bainite transformation should be examined during studying the mechanism of transformation. For upper bainite, it has been shown [90] that cementite, formed from carbon-enriched residual austenite, is not connected with the actual formation of bainitic ferrite. These carbides form as a result of the diffusional decomposition of austenite which remains untransformed after bainitic ferrite formation. In lower bainite, there are interplate carbides and intra-ferrite carbides. The formation of interplate carbides is the same in upper and low bainite, so that the intra-ferrite carbide precipitation in lower bainitic ferrite may have a critical role to play in the transformation mechanism itself. However, before this issue can be tackled, it is necessary to resolve whether lower bainitic carbides precipitate from a supersaturated ferrite matrix, or whether such precipitation can be described as "interphase precipitation" [100], or just precipitate from austenite during transformation. A rigorous crystallographic analysis [95] has confirmed that the expected three phase α-γ-θ relationship does not exist, and this is interpreted as evidence that an interphase precipitation mechanism does not operate. From electron microscopy observations [95] and the point of view that austenite can comfortably accommodate a large amount of carbon in solid solution compared with supersaturated ferrite, whose equilibrium carbon content is below 0.03 wt%, it seems therefore that not only do carbides nucleate within the ferrite, but the major part of their subsequent growth is accomplished by relieving carbon supersaturated ferrite.

1.6.4 Shape Change

The remaining characteristic feature of bainite formation is that transformation is accompanied by a shape change [89]. This shape change is an invariant plane strain (IPS) in which the broad (habit plane) face of the ferrite plate corresponds to the invariant plane. Thus, the shape change is similar to that found for martensite, and with a large shear component. This shear mechanism of transformation implies that there is an atomic correspondence between parent and product lattices, so it is expected that at least the substitutional element X/Fe atom ratio remains the same everywhere on bainite transformation. It has been estimated [100] that the strain energy of bainite, due to shape strain, is about 400 J/mol.

1.6.5 Atom-Probe Study

An imaging-atom-probe study of the austenite/bainitic-ferrite interface [101] has shown a uniform distribution of substitutional alloying element even at transformation interface. This direct evidence (on an atomic scale) also rules out the local equilibrium model, in

which a required composition spike exists at the interface. There is no solute segregation at the austenite/bainitic-ferrite interface, so solute drag models [102] cannot therefore be claimed to affect the growth of bainite either. It is noted that excess carbon in bainitic ferrite has been found in this direct detection [101].

1.6.6 Photo-Emission Electron Microscopy

The possibility of bainite growing by a paraequilibrium mechanism has been examined with hot-stage experiments in a photo-emission electron microscope [103], so that the individual sheaf of bainite could be directly resolved during transformation. It has been demonstrated that bainite does not grow under conditions of paraequilibrium; the growth rate as measured experimentally is many orders of magnitude higher than that expected from carbon diffusion control.

1.6.7 Thermodynamic Evidence

One of the outstanding problems associated with the study of transformations in steels is the determination of the carbon content of freshly formed bainitic ferrite. The difficulty arises because direct experimental measurements can only focus on the post-transformation composition, which need not correspond to that existing during growth itself. In particular, any carbon supersaturation in the ferrite can be relieved either by the precipitation of carbides within the ferrite or by the partitioning of carbon into the residual austenite by means of diffusion. Both of these processes can be very rapid, because of the high mobility of carbon in iron, especially at the temperatures where bainite forms.

There is, however, a way in which an indirect solution to this problem can be achieved. Consider the case where bainitic ferrite inherits the full carbon content of the parent austenite during transformation. The reaction should, in principle, go to completion since there is no diffusion necessary. In practice, the whole of the austenite grain does not transform instantaneously because of kinetic restrictions (e.g. heterogeneous nucleation); even if the first plate of bainite forms with full supersaturation, it has the opportunity to reject its excess carbon into remaining austenite. Any further increment of transformation is therefore associated with a lower free energy change, due to the higher carbon content of the austenite from which it has to form. Eventually, a stage is reached (the T'_0 curve)

[47,89,101] where transformation become thermodynamically impossible,* since the free energies of austenite and ferrite of the same composition become identical. Hence by monitoring the stage at which the transformation stops, it should be possible to deduce the level of carbon supersaturation in ferrite during growth. The formation of fully supersaturated ferrite requires the carbon content of the austenite to fall below that indicated by the T_0' curve. A less than full supersaturation would lead to transformation conditions closer to equilibrium and a correspondingly increased maximum possible degree of transformation; the terminal carbon content of the austenite would also be higher, and nearer to that given by the extrapolated Ae_3' phase boundary.

A lot of thermodynamic analysis [47,64,65,89,101,105] have been made in an attempt to understand the nature of the "incomplete reaction phenomenon". In this, the bainite reaction stops after a certain amount of transformation at a given temperature and ideally reaches zero transformation at the Bs temperature. Indeed, the incomplete reaction phenomenon can be useful in deducing the level of carbon-saturation that existed in the ferrite during growth. The data [48,65,84,95,99] have shown that the isothermal transformation of bainite stops far short of the Ae_3' curve but is in excellent agreement with the T_0 and T_0' curves. This provides strong evidence that the bainitic ferrite grows with the precise composition of the parent austenite (i.e., its growth is in essence martensitic).

It can therefore be concluded that the formation of bainite involves the propagation of displacive sub-units with a full carbon supersaturation, and partitioning of the carbon into the residual austenite occurs subsequent to transformation, rather than during the growth process.

1.6.8 Nucleation of Bainite

It is essential to obtain an indication of the amount of driving force (ΔF_N) necessary in order to ensure a detectable nucleation rate for bainite transformation. However current nucleation theories are not sufficiently established to enable the calculation of this quantity from first principles. Bhadeshia [100] has solved this problem by resorting to experimental data of Steven and Haynes [106]. The principle of analysis [100] is described as follows.

---

* The locus of such positions, as a function of isothermal transformation temperature defines the T_0' curve, where austenite and ferrite (with a certain amount of stored energy associated with transformation strains) of the same composition have equal free energy. The corresponding curve for stress-free austenite and ferrite of identical composition is conventionally called the T_0 curve [104]. The Ae_3' curve [47] may be similarly defined for growth involving the paraequilibrium partitioning of carbon (but not of substitutional alloying element). For plain carbon steels, it follows that the Ae_3' and Ae_3 curves are identical.

In alloy steels a pronounced bay appears in the time-temperature-transformation TTT curves. The flat top of the lower C curve corresponds to the temperature where a detectable nucleation rate (for ferrite formation with a shape change) first becomes possible, and also represents the transformation start temperature of Widmanstätten ferrite or bainite. The continuity of W_S and B_S with increasing carbon or alloy content has often been found in various treatments [107]. Bhadeshia [100] has used the extensive data of Steven and Haynes [106] which provides a rich source on the variation of the B_S (or W_S) temperature as a function of alloy composition, in order to calculate ΔF_N. In this analysis, the calculation of ΔF_N is under two circumstances - these are when the ferrite nucleates with the parent austenite carbon content, and when ferrite has an equilibrium carbon content; substitutional element partitioning is not allowed in either case. The results have shown (as shown in Fig. I.10) that the formation of a nucleus with the equilibrium carbon content is the true circumstance; the alternative hypothesis would lead to nucleation against a positive driving force for a few of the steels, or in other words there is insufficient driving force to account for nucleation involving the formation of fully supersaturated ferrite. Intuitively, the formation of a nucleus with an equilibrium carbon content seems more reasonable (irrespective of the carbon content of the ferrite at the growth stage) when we consider that the thermally activated development of an embryo to the critical nucleus size occurs through a large number of small scale fluctuations, rather than a sudden large fluctuation. Under such circumstances the rejection of the few carbon atoms that would be expected within the critical nucleus volume should be readily feasible.

Since the flat top of the lower C curve in TTT curves corresponds to the first temperature at which the nucleation of ferrite (which exhibits an invariant plane strain) first becomes possible [90], the above results suggest that the nucleation of both Widmanstätten ferrite and bainite is similar and involves the equilibrium partitioning of carbon [100].

In Fig. I.10b, the variation of ΔF_N with temperature can be understood if it is accepted that the method involved the calculation of the free energy change $\Delta F^{\gamma \rightarrow \gamma_1 + \alpha}$ (accompanying the formation of ferrite which at all times contains an equilibrium carbon content) necessary to give a certain constant, detectable nucleation rate (N), irrespective of the steel used [100]. Through nucleation theory,

$$N \propto \nu \exp(-\Delta F^*/RT) \qquad \text{(I.10)}$$

where ν = pre-exponential attempt frequency factor

ΔF^* = activation barrier

R = gas constant

$$\begin{aligned} \text{and} \quad -\Delta F^* &\propto RT \ln\left(\frac{N}{V}\right) \\ -\Delta F^* &\propto \beta T \\ \text{where} \quad \beta &= R \ln\left(\frac{N}{V}\right) \end{aligned} \tag{I.11}$$

It follows β is a constant since N is a constant irrespective of the steel used. β is expected to be negative, since the nucleation rate must be less than the attempt frequency. It has assumed [100,108] a linear dependence of activation energy on the chemical driving force as equation I.12:

$$\Delta F^* = \lambda_1 \Delta F^{\gamma \rightarrow \gamma_1 + \alpha} + \lambda_1 F_{st} + \lambda_2 \sigma + \lambda_3 \tag{I.12}$$

where λ_1, λ_2 and λ_3 are assumed constant characteristics of the lattice and of the nucleus, F_{st} is the strain enery per unit volume of the nucleus and σ is the interfacial energy per unit area. From equation I.11 and 12, it follows that

$$-\lambda_1 |\Delta F^{\gamma \rightarrow \gamma_1 + \alpha}| \propto |\beta| T - \lambda_1 |F_{st}| - \lambda_2 |\sigma| - \lambda_3 \tag{I.13}$$

so that $-|\Delta F^{\gamma \rightarrow \gamma_1 + \alpha}| \propto T$, as observed in Fig. I.10b. Therefore the curve can be assumed to be a universal curve expressing ΔF_N as a function of temperature, so that a detectable nucleation rate should only be possible in any particular steel if $|\Delta F^{\gamma \rightarrow \gamma_1 + \alpha}|$ for that steel exceeds $|\Delta F_N|$ at the temperature concerned.

1.6.9 Transition from Widmanstätten Ferrite to Bainite, and Bainite to Martensite

One of the outstanding problems in alloy steel design is to understand why the transformation of Widmanstätten ferrite, bainite and martensite do not necessarily occur in all steels. Bhadeshia [100] has used the concepts of the nucleation of ferrite (which exhibit an invariant plane strain) and stored energy due to shape change, and proposed an excellent model. This thermodynamic model is explained as follows.

For Widmanstätten ferrite and bainite transformation, the nucleation stage involves the equilibrium partitioning of carbon, but the subsequent growth depends on the free energy available for the transformation. Thus two different situations are to be considered - growth with equilibrium carbon partitioning (represented by $\Delta F^{\gamma \rightarrow \gamma_1 + \alpha}$) and growth with full carbon supersaturation (represented by $\Delta F^{\gamma \rightarrow \alpha_s}$), corresponding to the Widmanstätten ferrite and bainite respectively.

Letting F_1 = Stored energy per mole of Widmanstätten ferrite
F_2 = Stored energy per mole of bainite ferrite.

Widmanstätten ferrite will then form below the Ae_3 temperature when

$$|\Delta F^{\gamma\rightarrow\gamma_1+\alpha}| > F_1 \quad \text{(I.14a)}$$

$$|\Delta F^{\gamma\rightarrow\gamma_1+\alpha}| > |\Delta F_N| \quad \text{(I.14b)}$$

Because the driving force necessary for a detectable amount of nucleation (i.e., $|\Delta F_N|$) should always be greater than that necessary to sustain growth, $|\Delta F_N|$ will always exceed F_1 and condition (I.14a) becomes redundant, where F_1 = 50 J/mol.

Bainitic ferrite will form below the T_0 temperature when

$$|\Delta F^{\gamma\rightarrow\alpha_s}| > F_2 \quad \text{(I.14c)}$$

$$|\Delta F^{\gamma\rightarrow\gamma_1+\alpha}| > |\Delta F_N| \quad \text{(I.14d)}$$

However, for any steel where the Widmanstätten ferrite transformation precedes bainite formation, condition (I.14d) will probably be redundant. In the case of bainite formation, $|\Delta F_N|$ is always greater than F_2, where F_2 = 400 J/mol.

In Fig. I.11, steels A, B and C correspond to low, medium and high-alloy steels, as manifested in the relative amounts of transformation driving force available at any specified temperature. The driving force necessary for the athermal nucleation of martensite is indicated to be independent of temperature; such behaviour is approximately representative of martensitic transformation in steels [109]. For steel A, all three transformations (i.e., α_w, bainite and martensite) can occur. In steel B when $|\Delta F^{\gamma\rightarrow\gamma_1+\alpha}|$ become greater than $|\Delta F_N|$, $|\Delta F^{\gamma\rightarrow\alpha_s}|$ also exceeds F_2 so that the first shear transformation to occur would lead to bainite formation. Similarly steel C is expected to exhibit only martensite because above M_s temperature $|\Delta F_N|$ is larger than $|\Delta F^{\gamma\rightarrow\alpha_s}|$. The schematic free energy curves can illustrate why all three shear transformations need not occur in all steels.

1.7 Reaustenitisation

In multirun welds, the layers deposited initially are reheated by the deposition of subsequent layers (as shown in Fig. I.12), with a consequent modification of their microstructure. The volume fraction of the reheated zone depends on the number and the size of the beads deposited [110]. Actually some of the reheated zone of weld metal is involved in the process of reaustenitisation. Reaustenitisation is a complicated process, which has not been investigated widely in the past. This reaction is influenced by heating rate, chemical composition and starting microstructure. In this section, the literature on

reaustenitisation beginning with different starting microstructures is surveyed, although work on reaustenitisation from bainite does not seem to have been reported.

1.7.1 Reaustenitisation from Mixture of Ferrite and Pearlite

Investigation of the process of reaustenitisation from a ferrite and pearlite starting microstructure [111-119] have been stimulated by the development of "Dual-Phase Steels" (low carbon manganese steel containing about 1.5 wt% Mn), in which the steel is at least partially reaustenitised and then quenched to produce a mixed microstructure of ferrite and martensite. Most authors have pointed out that the nucleation of austenite seems to occur rather easily at pearlite-ferrite grain boundaries or at pearlite colony intersections, but not within the pearlite colonies. On the other hand, Navara et al. [119] recently studied austenite forming at a relatively low temperature close to the Ae_1 phase boundary, and proposed that the early stages of austenite formation at low temperatures involved the migration of ferrite boundaries with a zone being left behind the migrating boundary, enriched in the manganese concentration. They have suggested that this initial stage of austenite formation is associated with a manganese diffusion induced ferrite boundary migration [120-122]. However, the mechanism of diffusion induced grain boundary migration has not yet been established clearly and there is no work on diffusion induced interphase boundary migration. Although they claim that cementite particles did not play any role in the nucleation of austenite in the steels studied, they did not provide any microstructural evidence to establish the point.

Speich et al. [111] delineated the process of reaustenitisation in the $\alpha + \gamma$ phase field for such steels into three stages: (1) very rapid growth of austenite into pearlite until pearlite dissolution is complete; (2) slower growth of austenite into ferrite; and (3) very slow final equilibration of ferrite and austenite. These three steps are discussed as follows:

(1) Austenite Growth into Pearlite: The first step consists of pearlite dissolution and growth of austenite into the pearlite at a rate controlled primarily by carbon diffusion in the austenite, with the diffusion path lying along the pearlite-austenite interface, with a diffusion distance about equal to the interlamellar spacing of the pearlite. Generally, because of the very short diffusion distance involved, it is expected that the growth rate of austenite during this step will be extremely rapid, assuming that the processes of atom transfer across the interface is not rate limiting.

(2) Austenite Growth into Ferrite: After completion of the first step, or concomitant with it, the austenite will grow into the surrounding ferrite to achieve its equilibrium volume fraction given by the lever rule in the two-phase region. In this stage, the mechanism of austenite growth depends on the driving force for reaustenitisation. At high

austenitising temperatures close to the Ae_3 phase boundary, the driving force for reaustenitisation is high, and the transformation tends toward paraequilibrium or negligible-partitioning-local equilibrium. The concepts of paraequilibrium and negligible-partitioning-local equilibrium have been reviewed in Section 1.5. Paraequilibrium is a state of constrained equilibrium in which the substitutional lattice is configurationally frozen with respect to the transformation interface. Hence, even though the transformation is diffusional in nature, the ratio X/Fe (atom fraction of substitutional element/atom fraction of iron) is the same in ferrite and in austenite. Thus, the chemical potentials of the substitutional elements are not equal in the two phases. Carbon, which diffuses faster, reaches equilibrium subject to this constraint. In negligible-partitioning-local equilibrium (NP-LE), equilibrium is maintained for all species at the transformation interface, but the diffusion of substitutional alloying elements is extremely short-range, being confined to the immediate vicinity of the interface. Other than in the interface region, the concentration of substitutional element is essentially the same in all phases. At lower austenitising temperatures just above the Ae_1 phase boundary, the degree of supersaturation is decreased, and austenite transformation at a low supersaturation is that there is considerable partitioning and long-range diffusion of substitutional alloying element. However, the driving force for carbon diffusion is reduced to a level which allows the substitutional element flux to keep pace with the carbon flux at the interface. This situation is referred as the partitioning under local equilibrium condition (P-LE). The transition from paraequilibrium or NP-LE condition to P-LE condition as the degree of supersaturation is decreased is analogous to the reverse case where ferrite grows from austenite.

(3) Final Equilibration: In the final stage, the manganese concentration gradients within the austenite will be eliminated by diffusion within the austenite. The diffusivity of manganese in austenite is much slower than in ferrite. The time for completion of this process is extremely long.

There is some work [123-126] on reaustenitisation from a eutectoid pearlite structure. It has been found that nucleation of austenite in pearlitic structures occurs preferentially at the edges of the pearlite colonies on the cementite/ferrite boundaries (as shown in Fig. I.13). No evidence has been found for nucleation of austenite at the cementite interlamellar surfaces [125,126] within pearlite colonies. This is true even though the interfacial area per unit volume of lamellar cementite is many times larger than that of the cementite at the pearlite colony intersection. This is probably because the lamellar cementite sometimes has a Bagaryatskii orientation relationship with ferrite, so the interfacial energy may be lower, when compared with that of cementite at the pearlite colony intersections. Numerous observations [124,125] have shown that some lamellar

cementite still remains as the initial stages of austenitisation reach completion. This residual cementite may eventually dissolve or spheroidise depending on the transformation temperature.

1.7.2 Reaustenitisation of a Mixture of Ferrite and Spheroidal Cementite

The ferrite plus spheroidised cementite structure can be obtained by tempering martensite at a temperature just below the Ae_1 phase boundary. In this condition, the cementite particles end up primarily at the ferrite/ferrite grain boundaries, depending on the duration of the heat treatment. On the other hand, if the material is subsequently heavily cold-deformed and recrystallised at a temperature just below Ae_1 again, then a structure in which almost all the spheroidised cementite particles are dispersed in the ferrite matrix away from the ferrite grain boundaries, can be obtained. Such a "strain-anneal" technique has been used [125,127] in order to study whether ferrite grain boundaries have any effect on the nucleation of austenite. It has been confirmed [112,125,127] that the nucleation of austenite in ferrite plus spheroidised cementite structure preferentially occurs at junctions between the cementite particles and ferrite grain boundaries. This is due to the surface energy contribution to the bulk free energy necessary for the formation of stable austenite nuclei. The energy contribution results when the austenite nucleus replaces a small segment of an α/α boundary. Speich et al. [125] also suggested that the density of carbides in the ferrite grain boundaries essentially controlled the number of nucleation events or initial austenite grain size.

In the initial stages of reaustenitisation, the growth of the austenite across the α/α boundaries is inhibited and eventually the austenite film grows around the spheroidised cementite particle to completely envelope the cementite before an appreciable part of the dissolution process has occurred [125,127]. Further growth of the austenite can occur by carbon diffusing from the dissolving cementite to the austenite envelope. During this stage, a more informative approach to the problem of austenitisation would be to determine the mechanism that controls the rate of dissolution of carbide in austenite and how it is modified by alloying elements. Hillert et al. [128] studied the effect of alloying elements on the formation of austenite and the dissolution of cementite, and proposed that during the austenitisation, local equilibrium is established at the cementite/austenite interface, and that the growth rate of austenite (or dissolution rate of cementite) is governed by the diffusion of carbon and other substitutional elements in austenite. After cementite particles located on ferrite grain boundaries are dissolved in the shell of austenite, the austenite grains grow both away from and, more significantly, along the ferrite boundaries. Nemoto [123] conducted in situ experiments using a high voltage electron microscope, and argued that during austenitisation, mobile austenite-ferrite

interfaces are attracted to cementite particles in ferrite matrix. Once the austenite grain has made contact with that cementite particle, the dissolution will accelerate and the austenite grain will grow rapidly around the particle. This seems to provide evidence that the cementite particles which originally resided in the ferrite matrix do not contribute to austenite nucleation [112].

1.7.3 Reaustenitisation of Martensite

Reaustenitisation of martensite has been studied in dual-phase (ferrite/martensite) steels. These are a new class of high-strength low-alloy sheet steels that have superior combinations of strength and uniform ductility. Thomas et al. [131] have used different heat treatment processes to study the microstructures and the mechanical properties of dual-phase steels, and suggested that dual-phase steels with optimum properties can be obtained when the starting structure is martensite. These steels are produced by heating the martensite in the $\alpha+\gamma$ phase region and then quenching to ambient temperature. During isothermal heat treatment in the $\alpha+\gamma$ field, islands of austenite form, and on quenching, this austenite transforms to martensite in a matrix of equiaxed ferrite. It has been found that there are two types of austenite morphology, called globular and acicular austenite* [132-137], forming from the starting martensitic microstructure. Koo et al.[132] have presented a heat treatment process (as shown in Fig. I.14) to produce controlled dual-phase structures (as shown in Fig. I.15). In Fe-0.5Cr-0.1C (wt%) dual-phase steel (Fig. I.15b), globular austenite particles exhibit a continuous network along the prior austenite grain boundaries with the acicular austenite particles within the prior austenite grains. However, there is a significant change in the morphology of austenite as chromium content increases. For example, Fe-4Cr-0.1C (wt%) dual-phase steel (as shown in Fig. I.15a), globular austenite particles not only continuously decorate prior austenite grain boundaries but also display within the austenite grains. Finally they have shown that in a Fe-2Si-0.1C (wt%) dual-phase steel (as shown in Fig. I.15c) the microstructure exhibits a fine, fibrous and discontinuous distribution of acicular particles in the ferrite matrix. It is seen that the influence of the starting martensitic structure is clearly reflected in the last case. The alloying element effects on these austenite morphologies will be discussed later.

The formation of austenite from martensite may occur by classical heterogeneous nucleation [138] at such lattice imperfections as prior austenite boundaries, martensite lath boundaries and matrix/carbide interfaces etc. The dominating influence of boundaries in the austenite nucleation process arises from the reduced activation energy for nucleation at the boundaries, as predicted by classical nucleation theory. However, some attention

---

* "Acicular austenite" grows along the original martensite boundaries, and the plates of austenite appear to have parallel habit planes within a packet of what was originally martensite. Acicular ferrite nucleates from inclusions in weld deposits, and its morphology consists of non-parallel plates of ferrite.

should be given to the role of substructural features in martensite in order to fully establish the mechanism that leads to the preferential nucleation in a martensitic structure. First of all, concerning the presence of retained austenite trapped between martensite laths, these sites may be preferred for nucleation because of the presence of the transformation products formed when retained austenite in the original microstructure decomposes during heating to the reaustenitisation temperature. That is, during heating of the martensitic structure into the two phase region, the retained austenite may decompose into ferrite and carbides. These carbides would be located at the lath boundaries and can provide active sites for austenite nucleation. On the other hand, if retained austenite remains stable on heating into the $\alpha+\gamma$ region, then the reaustenitisation involves only the growth of extant austenite. The relative significance of retained austenite in this process remains unknown. The other feature which may also have to be taken into account is the auto-tempered carbide which is sometimes present within martensite. Speich et al. [125,127] have shown that while austenite nucleation occurs preferentially at the carbides located at grain boundaries, it does not do so at the carbide present in the matrix. Hence auto-tempered carbides probably do not provide sufficient nucleation sites to compete with the other favourable sites for austenite nucleation.

The influence of alloying elements on the growth pattern of austenite from the starting martensitic structure is very important. Koo et al. [132] have suggested that a fine scale, discontinuous, and fibrous distribution of "acicular" austenite particles (becoming martensite after final quenching) is a desirable microstructure with optimum properties. There is some work [133,139] on the influence of alloying elements upon the morphology of austenite formed from martensite, However, the mechanism for the morphological changes is not clear. Plichta et al. [133] classified many ternary Fe-X-C systems (X being substitutional alloying element) into three groups according to the observed morphology of the dual-phase microstructure. In their work, the view is expressed that competitive processes between the nucleation and growth of austenite at lath boundaries and the migration of these boundaries determine the final product shape. More specifically, according to their explanation, rapid migration of the lath boundaries compared to the kinetics of austenite formation results in the globular shape of austenite. On the other hand, they argue that the high rate of austenite nucleation will restrict the lath boundary migration, thereby ensuring the growth of acicular austenite. They further argue that the globular shape of the austenite particles in Fe-Cr-C dual-phase steels can be attributed to a solute drag effect [102] upon growth. However, their explanations are inconclusive. For example, they have not recognised the drastic change in morphology that occurs as a function of alloying element concentration. An "acicular" shape of austenite was observed in a Fe-0.5Cr-0.1C (wt%) dual-phase steel, where, as a globular morphology was obtained in a Fe-4Cr-0.1C(wt%) dual-phase steel.

It is believed that during reaustenitisation, a local equilibrium may be established at the γ/α boundaries. In this condition, substitutional elements may be required to diffuse for a short distance depending on the driving force of reaustenitisation. This idea basically leads to the presence of a narrow concentration "spike" just ahead of and in contact with the advancing boundary. The existence of such a narrow concentration "spike" has been considered in negligible-partitioning local equilibrium (NP-LE), as discussed in Section 1.5.

Assuming the presence of the concentration "spike", it becomes obvious that the kinetics of γ/α boundary migration should be influenced strongly by the type of alloying element present in the dual-phase steels. The microstructures (as shown in Fig. I.15), which Koo et al. [132] have presented for Fe-2Si-0.1C (wt%), Fe-0.5Cr-0.1C (wt%) and Fe-4Cr-0.1C (wt%) dual-phase steels, may qualitatively be explained as follows. In the case of Si steels, the Si concentration "spike" will act as a barrier to carbon diffusion from ferrite to austenite because of the repellent interaction between silicon and carbon atoms [140]. As a result, once austenite nucleation occurs, the lateral thickening of the austenite particles at the lath boundaries will be restricted, and austenite grows in an acicular manner along the lath boundaries, clearly reflecting the starting martensitic structure. In the case of Fe-0.5Cr-0.1C steel, the influence of the boundary diffusion process may overcome the effect of the concentration "spike" with a result that austenite particles grow predominantly along the lath. This situation is entirely changed as the concentration "spike" becomes higher, and hence more influential with increased chromium content. In the case of Fe-4Cr-0.1C steel, the dominating effect of the "spike" on carbon diffusion encourages three-dimensional growth, resulting in the globular shape of austenite particles. This concentration "spike" model seems to be able to explain the observed alloying element effect. It needs further fundamental studies to clarify the role of alloying elements on transformation kinetics.

1.8 The Heat Affected Zone

When base plates are joined by fusion welding, the material of the plates near the fusion boundary is heated to its melting point and then cooled rapidly under conditions of restraint imposed by the geometry of the joint. As a consequence of this severe thermal cycle the original microstructure of the base metal in a region close to the weld is changed; this microstructure is usually referred to as the heat affected zone (HAZ). Experience has show that failures occur frequently in the HAZ. Much work has been devoted to correlating the presence of unfavourable microstructures and the various failure modes that are obtained. Although some work has been done [141-146] on the study of microstructures in the HAZ, a model for predicting the microstructure has not been developed as yet.

The microstructure of the HAZ is influenced by both the peak temperature which determines the austenite grain size and the cooling time over the temperature range 800 → 500°C. Ashby and Easterling [141] have presented a schematic diagram (as shown in Fig. I.16) to divide the HAZ of a single run weld (alternatively the capping layer of a multirun weld) into a number of sub-zones for plain carbon steel. Each zone is characterised by a specific peak temperature (T_p) interval:

(i) solid-liquid transition zone: Tp close to the melting point;
(ii) coarse austenite grain zone: 1100°C < T_p < 1450°C;
(iii) austenite grain refined zone: Ar_3 < T_p < 1100°C;
(iv) partially transformed zone: Ar_1 < T_p < Ar_3; and
(v) tempered zone: Tp below Ar_1.

Each sub-zone refers to a different type of microstructure and, perhaps more importantly, each type of structure possesses different mechanical properties. For instance, the larger austenite grain size can shift the CCT curve to longer reaction times producing more Widmanstätten ferrite, or increasing the possibility of martensitic or bainitic transformation products on cooling. This, together with the larger grain size, may lower the toughness and increase the risk of hydrogen cracking* [147]. The structure type and its sub-zone width are determined by the thermal cycle, i.e., the complete cycle of heating and cooling due to the movement of the arc and the thermal properties of the base metal. However, the prior thermal and mechanical history of the material are very important factors as well. For example, the recrystallisation behaviour during the heating cycle is affected by whether the original material was in cold rolled or annealed condition prior to welding. In microalloyed steel base plate, the onset and extent of the grain growth are influenced by the presence of precipitates and their solubility at high temperature. Thus in order to obtain a reasonable understanding of the HAZ, it is necessary to consider the whole range of phase transformations in the complete thermal cycle.

1.8.1 The Temperature Profiles

With the aim of predicting thermal cycles, most studies of heat flow in HAZ has been undertaken in two discrete areas: computation and direct measurement. Some research [141,143,145] has led to the calculation of the temperature/time profiles in the heat affected zone using the theory of Rosenthal [148], which is found to give a good

* The main source of hydrogen in welding arises from the dissociation of water vapour in the welding arc. The solubility of hydrogen in austenite is much higher than in ferrite. Therefore, as the transformation $\gamma \rightarrow \alpha$ proceeds the austenite becomes progressively more enriched in hydrogen. This may be the reason why cold cracking is so sensitive to the presence of martensite, since the martensite transformation occurs at the lowest temperature and originates from the most hydrogen enriched austenite.

description of the actual thermal cycle. The equations give the temperature T {r,t} at a point lying a distance r from the weld centre-line, as a function of time t, caused by a point heat source moving with velocity υ across the surface. The temperature rises to a peak T_p, and then falls, the time to drop from 800 to 500°C being designated Δt. Two limiting solutions are used. For thick plates, and assuming an instantaneous application of heat, we have [143]

$$T = T_e + \frac{q/\upsilon}{2\pi\lambda t} \text{Exp}(-\frac{\gamma^2}{4at}) \quad \text{(I.15a)}$$

$$Tp = T_c + \frac{2}{\pi e} \frac{q/\upsilon}{\rho c r^2} \quad \text{(I.15b)}$$

$$\Delta t = \frac{q/\upsilon}{2\pi\lambda} \{ \frac{1}{773 - T_c} - \frac{1}{1073 - T_c} \} \quad \text{(I.15c)}$$

while for a thin plate, for an instantaneous application of the heat

$$T = T_c + \frac{q/\upsilon}{d(4\pi\lambda\rho ct)^{1/2}} \text{Exp}(-\frac{\gamma^2}{4at}) \quad \text{(I.16a)}$$

$$Tp = T_c + (\frac{2}{\pi e})^{1/2} \frac{q/\upsilon}{2d\rho cr} \quad \text{(I.16b)}$$

$$\Delta t = \frac{(q/\upsilon d)^2}{4\pi\lambda\rho c} \{ \frac{1}{(773 - T_c)^2} - \frac{1}{(1073 - T_c)^2} \} \quad \text{(I.16c)}$$

Here q is the arc power, υ the arc speed, e base of natural logarithms = 2.718, λ the thermal conductivity, ρ the density, c the specific heat, a the thermal diffusivity, T_c the preheat temperature and d the plate thickness.

It has found [143] that in the case of thick plates, if the point source of heat is replaced by a circular disc source, the Rosenthal equations can provide a better approximation to arc welding processes. In the case of the HAZ of multirun welds, the effect of superimposition of successive weld thermal cycles on the temperature profile is much more complicated, and much further research is necessary.

1.8.2 Phase Transformations in the HAZ

During the heating cycle, there are several processes occurring in the HAZ, such as $\alpha \rightarrow \gamma$ transformation, pearlite/cementite $\rightarrow \gamma$ transformation, carbon redistribution in austenite, precipitate (carbonitride) coarsening, precipitate dissolution, austenite grain growth etc. It should be noted that the heating rate is extremely high near the fusion boundary; for example, in normal arc welding it can be of the order of about 200 ~

300°C per second [149], and the continuous heating transformation behaviour will be strongly influenced. This implies that the phase transformations are likely to be affected by the considerable superheating. However, there is little work [150,151] in this area, and further studies are called for. As to the grain growth of austenite, Ion et al. [143] have assumed that grain growth is driven by surface energy. The rate of austenite growth at a fixed temperature T is then given by

$$\frac{dg}{dt} = \frac{k_1}{2g} \exp\left(-\frac{Q}{RT}\right) \tag{I.17a}$$

and the grain size g, after time t is

$$g^2 - g_o^2 = k_1 t \exp\left(-\frac{Q}{RT}\right) \tag{I.17b}$$

where g_o is the initial size, k_1 is a kinetic constant and Q an activation energy. In a weld thermal cycle, the temperature varies with time. Then the grain size g after the cycle is related to the initial grain size g_o by

$$g^2 - g_o^2 = k_1 \int_o^{\infty} \exp\left(\frac{-Q}{RT\{t\}}\right) dt \tag{I.17c}$$

and the relation between final austenite grain size and peak temperature can be calculated. In the case of microalloyed steels, the austenite grain growth is partially controlled by a dispersion of fine precipitates (carbonitrides) which effectively pin the grain boundaries. During the heating cycle the particles coarsen or dissolve depending on the peak temperature, the input energy of the process and the composition of the particles. These problems are very complicated, and need more research [152].

Actually, the grain growth equation should be written as:

$$g^{1/n} - g_o^{1/n} = k_1 \int_o^{\infty} \exp\left(\frac{-Q}{RT\{t\}}\right) dt \tag{I.18}$$

and the prediction of the HAZ austenite grain size on the basis of equation I.18 presupposes that average values of both the time exponent n and the corresponding activation energy Q are available. For most metals and alloys, n varies typically in the range from 0.1 to 0.4 (depending on temperature and composition) even in the absence of effective grain boundary pinning precipitates [153,154]. Only in the case of ultrapure metals annealed at very high temperatures the time exponent n may approach a constant value of 0.5 [154]. In principle, an estimate of n and Q could be obtained from isothermal grain growth experiments [155], but such data are not necessarily representative of the conditions prevailing in a weld HAZ and are likely to be specific to certain alloys. An

additional requirement is that these parameters are essentially constant over a relatively wide temperature range, which clearly is not always met. Although the former problems to some extent can be overcome by the choice of an appropriate calibration technique [143] (i.e., selecting n = 0.5 and fitting the integrals at fixed points to specific data through adjustment of Q), an experimental verification of the various approximations involved is still lacking. More work will be needed in order to predict the grain size of austenite.

During the cooling cycle, the austenite transformation kinetics depend on austenite grain size and chemical composition. The allotriomorphic ferrite usually forms first along the austenite grain boundaries on cooling, and pearlite, Widmanstätten ferrite, bainite and martensite form later. More work is needed to rationalise quantitatively the grain size effect on this part of transformation cycle.

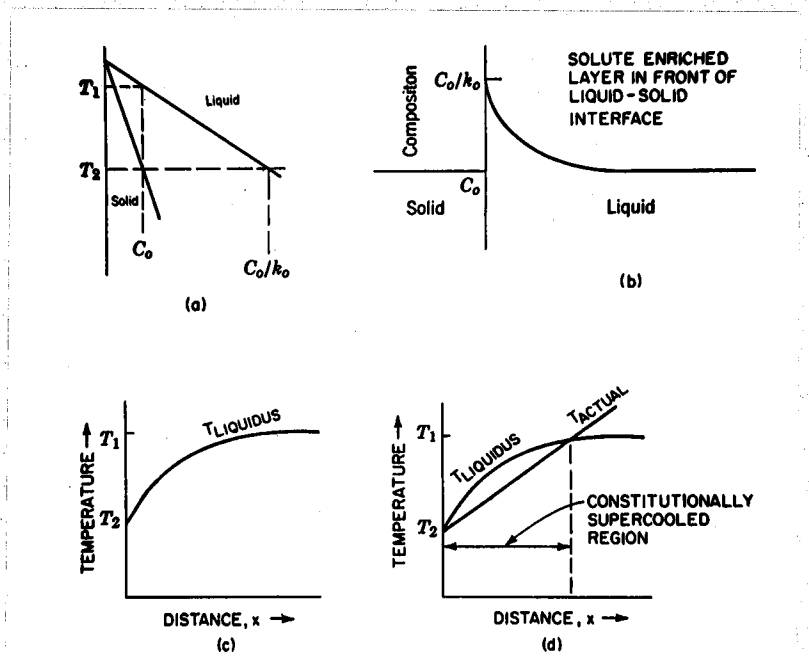

Figure I.1 - Constitutional supercooling in alloy solidification. (a) Phase diagram; (b) solute-enriched layer in front of solid-liquid interface; (c) liquidus versus distance from solid-liquid interface; (d) constitutional supercooling layer.

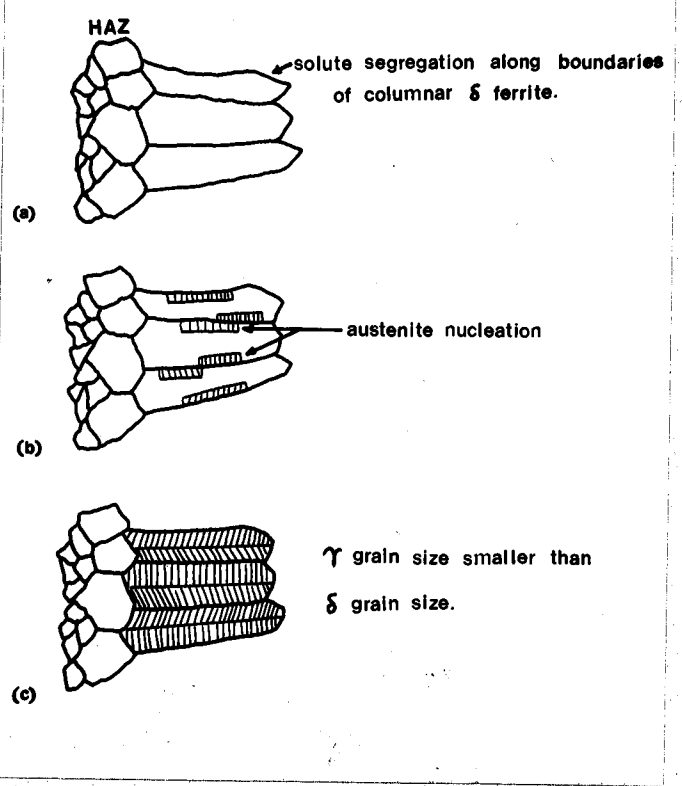

Figure I.2 - The solidification sequence for low carbon steel weld metal deposit.

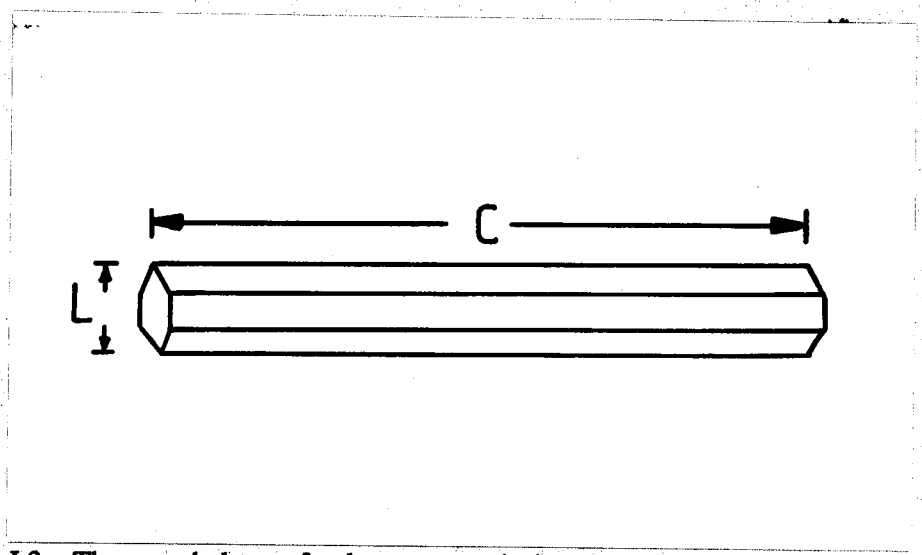

Figure I.3 - The morphology of columnar γ grain is represented by a hexagonal prism.

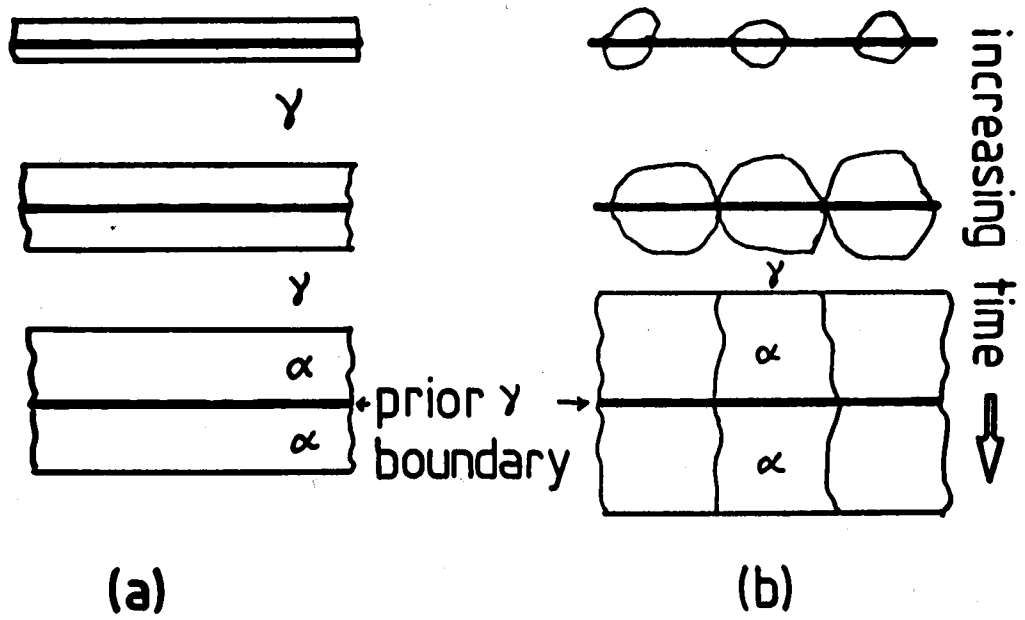

Figure I. 4 - Diagram illustrating the growth of allotriomorphic ferrite as (a) the normal migration of planar γ/α interface, and as (b) is the case of reality. (After Bhadeshia[39]).

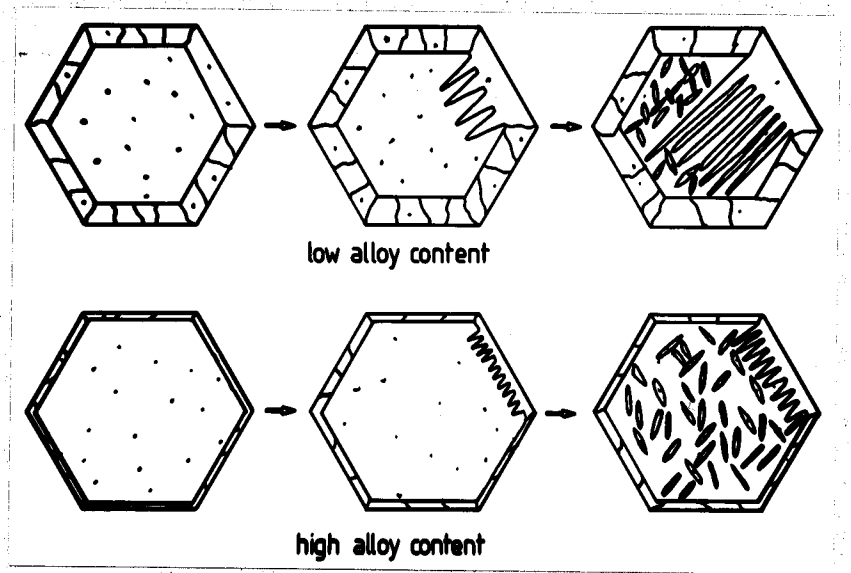

Figure I.5 - Schematic diagrams shows the development of microstructure in weld deposits. (after Bhadeshia et al.[1]).

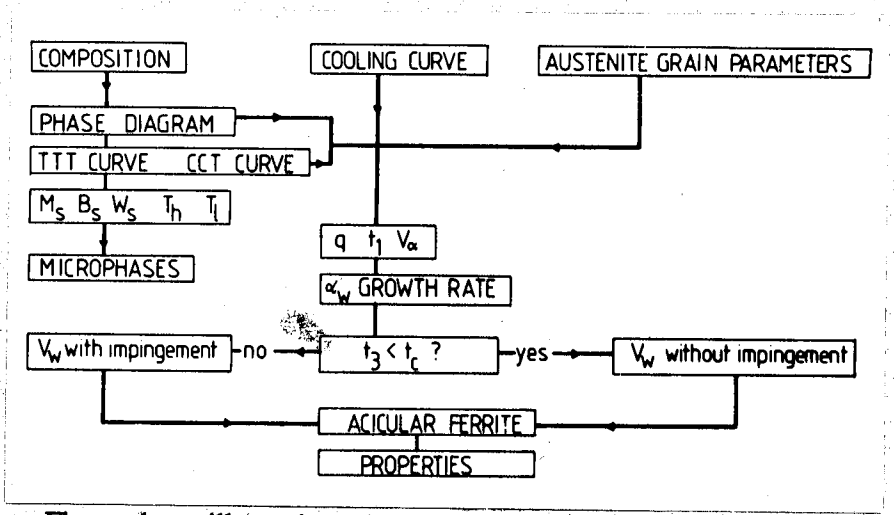

Figure I.6. - Flow chart illustrating the steps involved in the calculation of the microstructure. (after Bhadeshia et al.[1]).

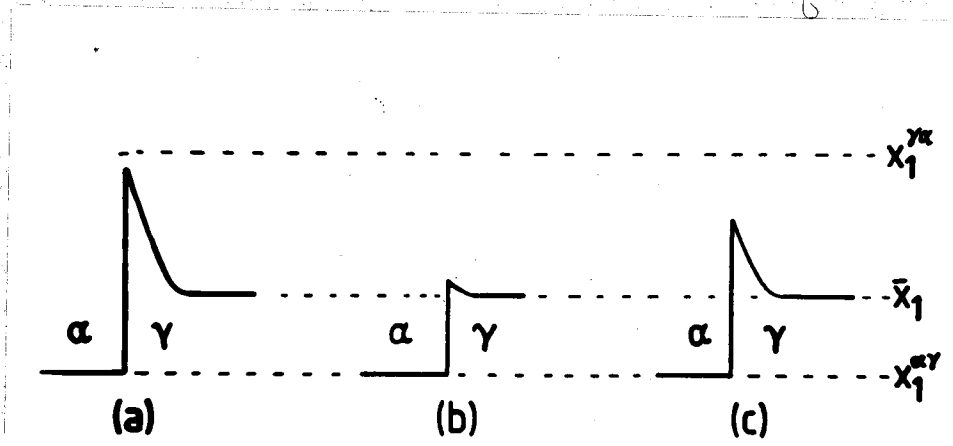

Figure I.7 - Carbon concentration profile at γ/α interface moving under: (a) diffusion-control; (b) interface-control; and (c) mixed interface and diffusion-control.

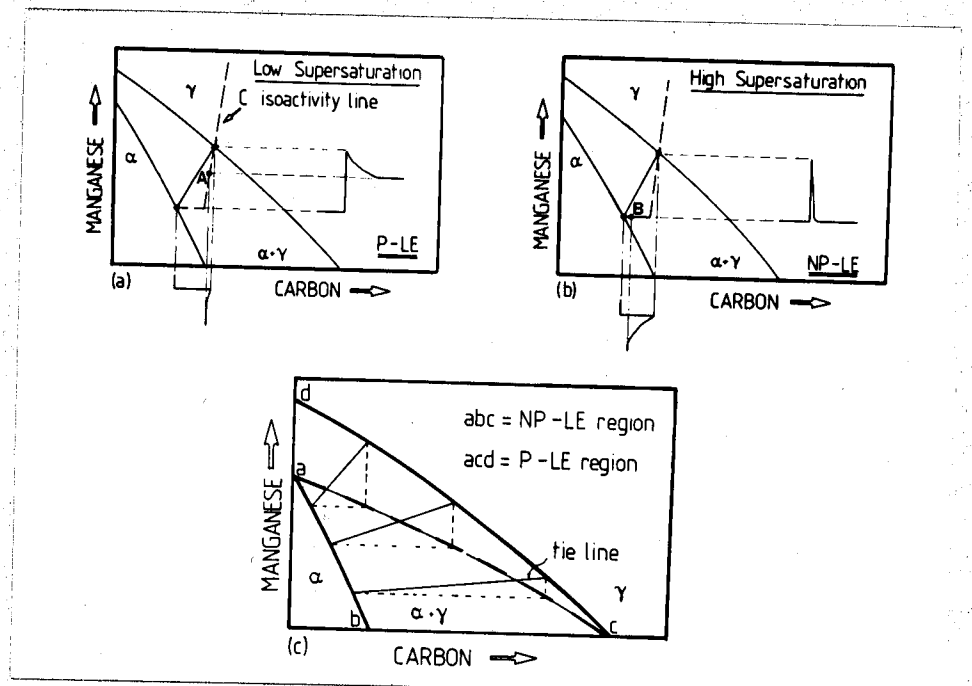

Figure I.8 - Schematic isothermal sections of the Fe-Mn-C system, illustrating ferrite growth occurring with local equilibrium at the α/γ interface. (a) Growth at low supersaturations (PLE) with bulk redistribution of Mn, and (b) growth at high supersaturations (NPLE) with negligible partitioning of Mn during transformation. The bulk alloy compositions are designated "A" and "B" in Fig. I.8(a) and (b) respectively, and (c) division of the $\alpha + \gamma$ phase field into domains where either the PLE or the NPLE mechanisms can operate.

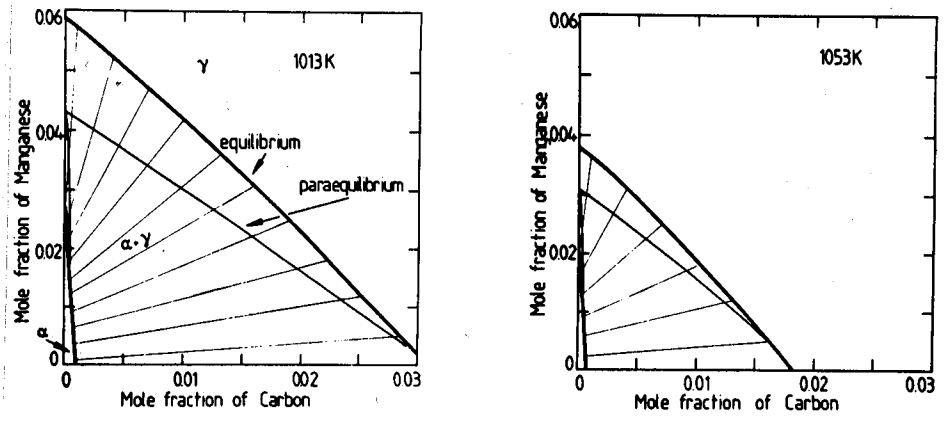

Figure I.9 - Typical calculated isothermal sections of the equilibrium and paraequilibrium phase diagrams of the Fe-Mn-C system (after Bhadeshia[25]). The tie-lines for the paraequilibrium diagram are virtually horizontal since the Fe/Mn ratio is constant everywhere during paraequilibrium transformation.

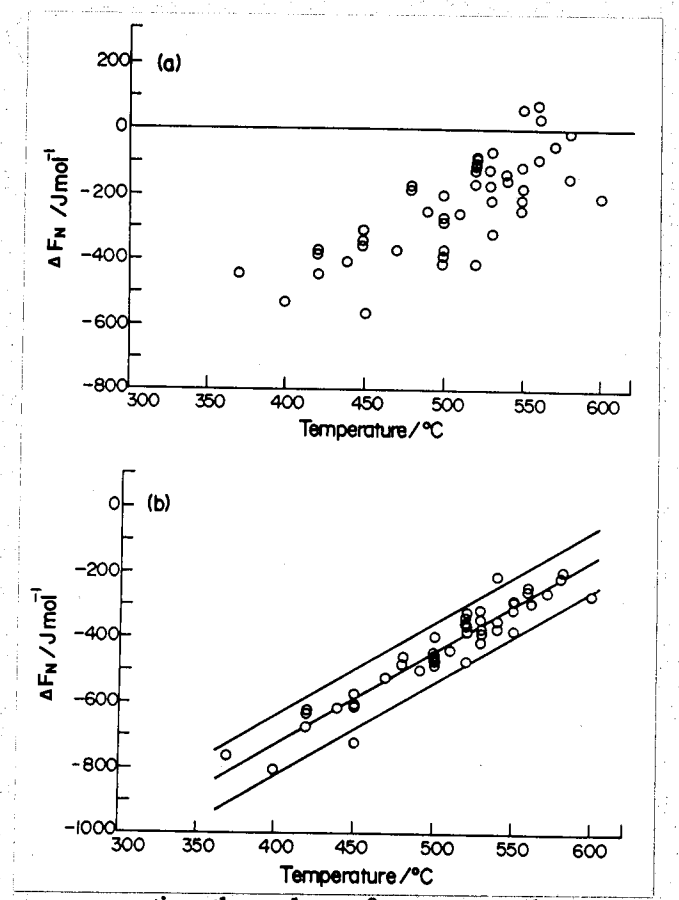

Figure I.10 - Curves representing the volume free energy change necessary in order to obtain a detectable nucleation rate for ferrite forming by shear. (a) The case when the volume free energy change is calculated on the basis that the ferrite nucleus inherits the parent austenite carbon content. (b) The case when the volume free energy change is calculated on the basis that the ferrite nucleus at all times contains only an equilibrium carbon content. The lines bounding the regression line are vertically spaced at distances equivalent to two standard errors of the estimate from the regression line (after Bhadeshia[100]).

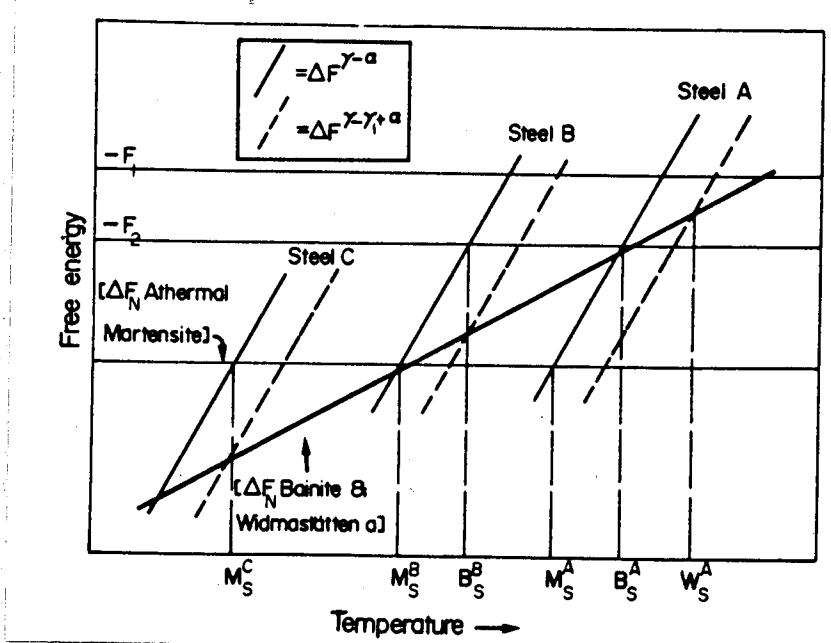

Figure I.11 - Schematic free energy curves illustrating why all three shear transformations need not occur in all steels (after Bhadeshia[100]). It is noted that F_1 = 50 J/mol, for stored energy of α_w. F_2 = 400 J/mol, for stored energy of α_b, and ΔF_N, $\Delta F^{\gamma \rightarrow \alpha}$s and $\Delta F^{\gamma \rightarrow \gamma_1 + \alpha}$ all are negative.

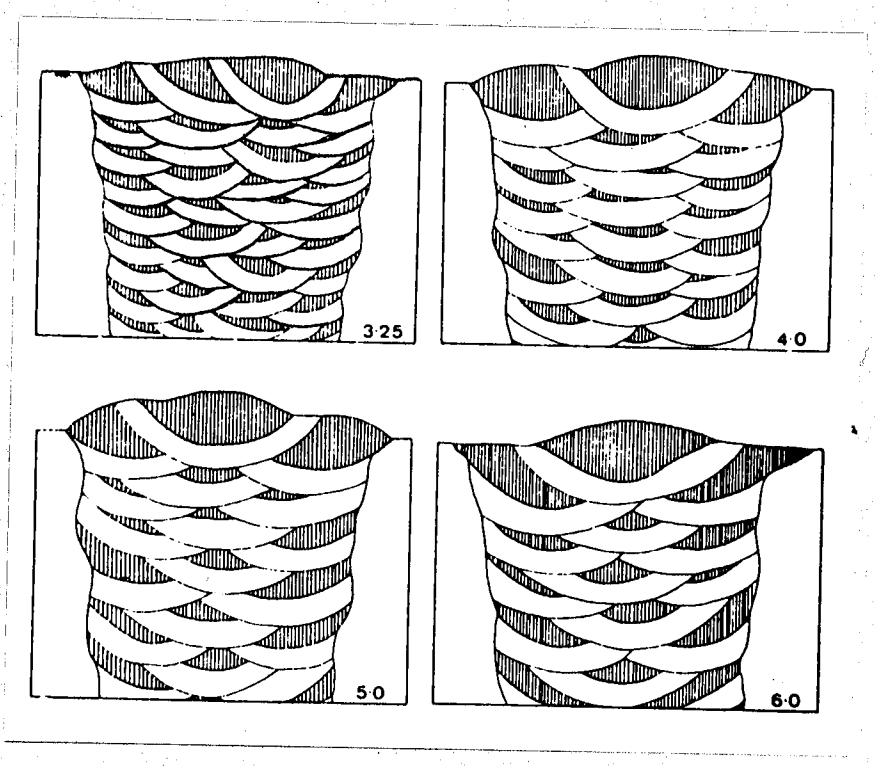

Figure I.12 - Schematic diagram shows the deposition layers and the reheated zones (the white areas) in multirun welds of different electrode sizes (after Evans[110]). The electrode diameters (in mm) are given in the bottom right hand corners of each figure.

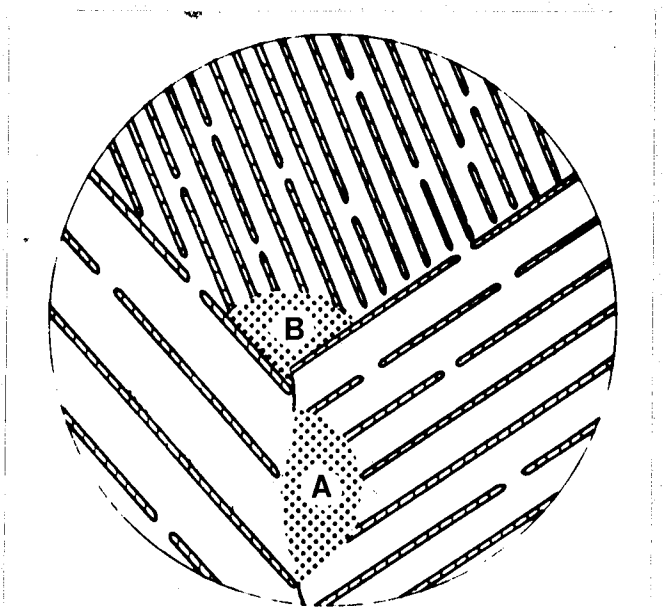

Figure I.13 - Schematic figure shows that preferential nucleation sites of austenite (A) and (B) are located at the edges of pearlite colonies on the cementite/ferrite boundaries (after Roosz[126]).

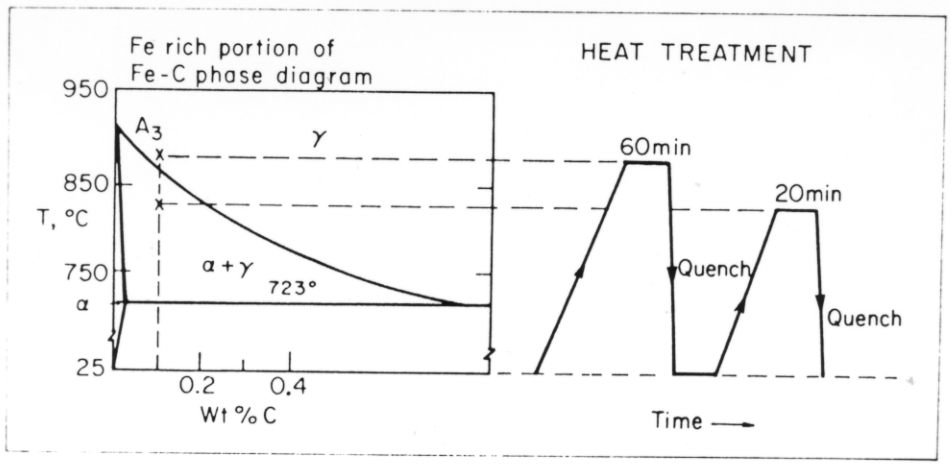

Figure I.14 - Schematic representation of heat treatment to produce controlled dual-phase (ferrite/martensite) structures. (after Koo[132]).

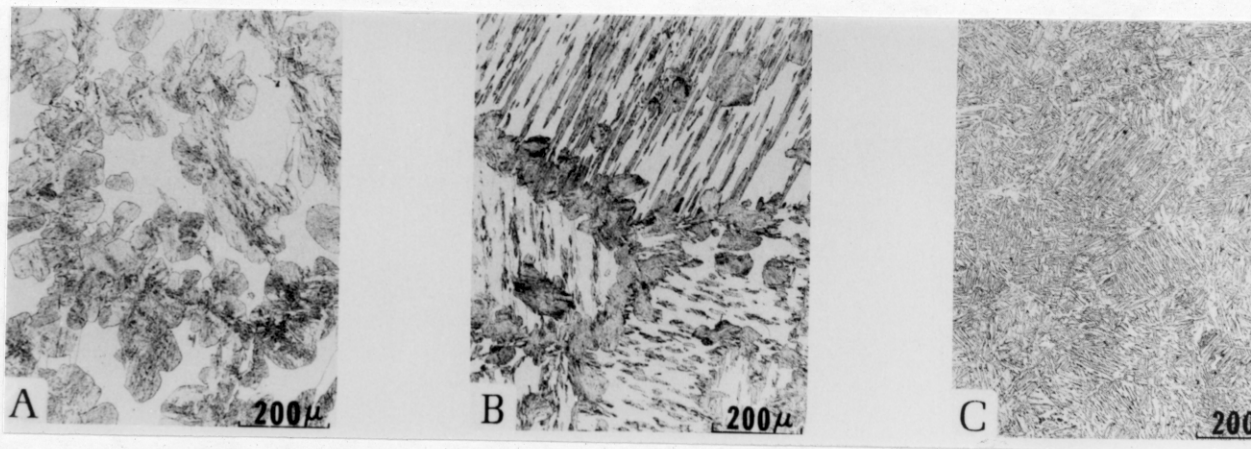

Figure I.15 - Optical Micrographs. (a) Dual-phase microstructure developed in Fe/4Cr/0.1C (wt%) steel shows the globular shape of martensite in the ferrite matrix. (b) Dual-phase microstructure developed in Fe/0.5Cr/0.1C (wt%) steel shows that acicular shape of martensite within prior austenite grain and the prior austenite grain boundaries are decorated with continuous globular shape of martensite particles. (c) Dual-phase microstructure developed in Fe/2Si/0.1C (wt%) steel shows fine, acicular shape of martensite particles in ferrite matrix. Note that martensite was austenite before final quenching. (after Koo[132]).

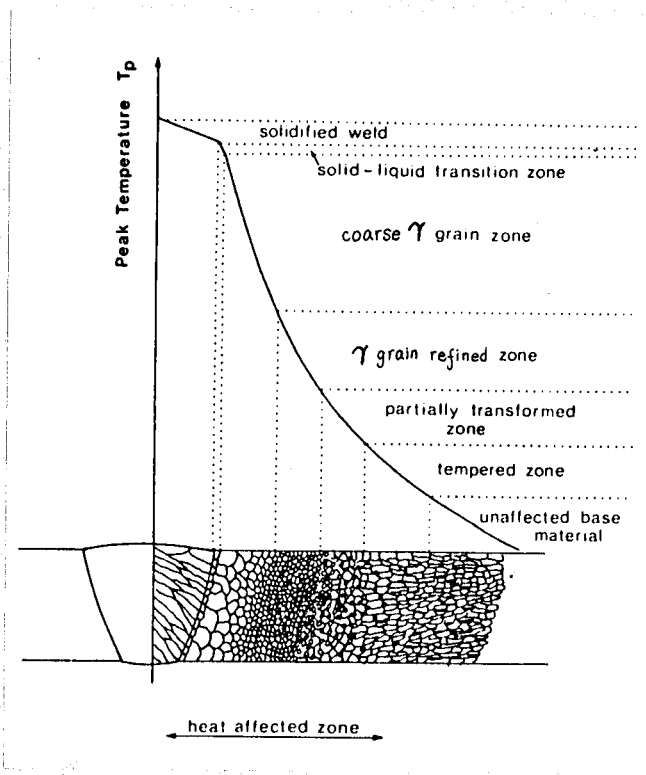

Figure I.16 - A schematic diagram shows various sub-zones of the heat affected zone in a plain carbon steel.